Safety Evaluation of J-turn Intersections in Missouri

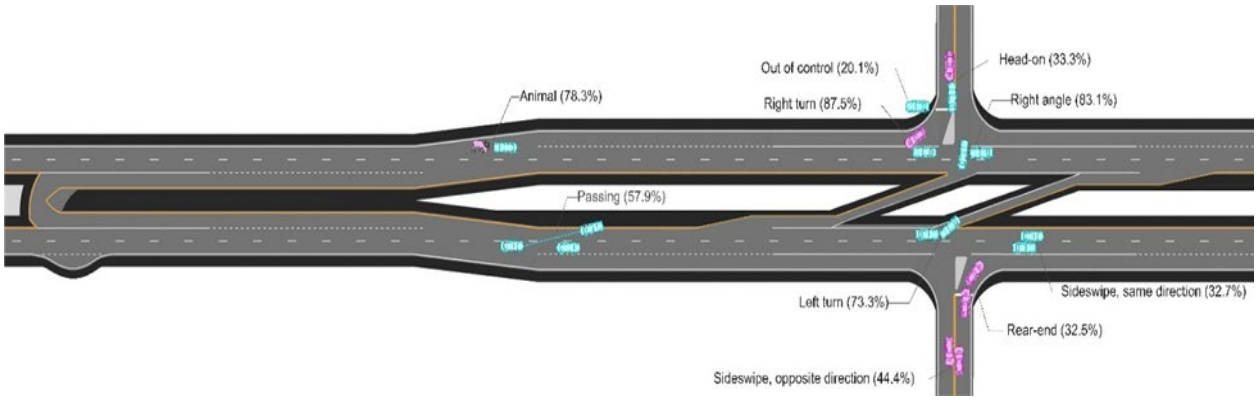

August 2024
Final Report

Project number TR202320
MoDOT Research Report number cmr 24-011

PREPARED BY:

Praveen Edara

Zhu Qing

Henry Brown

Carlos Sun

Ho Jun Baek

University of Missouri-Columbia

PREPARED FOR:

Missouri Department of Transportation

Construction and Materials Division, Research Section

TECHNICAL REPORT DOCUMENTATION PAGE

1. Report No. cmr 24-011	**2. Government Accession No.**	**3. Recipient's Catalog No.**
4. Title and Subtitle Safety Evaluation of J-turn Intersections in Missouri		**5. Report Date** July 2024 Published: August 2024 **6. Performing Organization Code**
7. Author(s) Praveen Edara, https://orcid.org/0000-0003-2707-642X Zhu Qing, https://orcid.org/0000-0002-3219-6971 Henry Brown, https://orcid.org/0000-0003-1473-901X Carlos Sun, https://orcid.org/0000-0002-8857-9648 Ho Jun Baek, https://orcid.org/0000-0001-6392-2385		**8. Performing Organization Report No.**
9. Performing Organization Name and Address Department of Civil and Environmental Engineering University of Missouri-Columbia E2509 Lafferre Hall Columbia, MO 65201		**10. Work Unit No.** **11. Contract or Grant No.** MoDOT project # TR202320
12. Sponsoring Agency Name and Address Missouri Department of Transportation (SPR-B) Construction and Materials Division P.O. Box 270 Jefferson City, MO 65102		**13. Type of Report and Period Covered** Final Report (January 2023-July 2024) **14. Sponsoring Agency Code**

15. Supplementary Notes

Conducted in cooperation with the U.S. Department of Transportation, Federal Highway Administration. MoDOT research reports are available in the Innovation Library at https://www.modot.org/research-publications.

16. Abstract

The design of J-turn intersections has gained its prevalence in Missouri due to their demonstrated safety benefits. However, with the growing number of J-turns and the availability of more crash data, there is a renewed need to deepen the understanding of the safety performance of J-turns. This study presents a comprehensive safety evaluation of J-turn intersections, analyzing their effectiveness in reducing total and fatal & injury crashes using crash data from 47 J-turn intersections between 2005 and 2021. Employing a robust methodology including both comparison group and empirical Bayes analyses, this study assesses the impact of J-turns on crash reductions compared to traditional two-way stop-controlled intersections. Two methods were used because they had different tradeoffs such as data requirements, simplicity of implementation, and regression to the mean. The comparison group analysis revealed reductions of 46.6% in fatal and injury crashes and 44.4% in total crashes. Similarly, the empirical Bayes analysis supported these safety improvements, showing reductions of 51.4% in fatal and injury crashes and 40.3% in total crashes. Furthermore, crash frequency models developed for Missouri's J-turn sites indicate that site characteristics such as loons, deceleration/acceleration lanes, and islands contribute to reduction in crashes. The study also includes detailed collision diagrams that outline crash locations and types at J-turn sites. The study findings provide insights and tools for MoDOT engineers as they consider J-turn design as a safety countermeasure at two-way stop-controlled intersections on rural highways.

17. Key Words J-turn, Safety benefit, Crash modification factor	**18. Distribution Statement** No restrictions. This document is available through the National Technical Information Service, Springfield, VA 22161.

19. Security Classif. (of this report) Unclassified.	**20. Security Classif. (of this page)** Unclassified.	**21. No. of Pages** 69	**22. Price**

Safety Evaluation of J-turn Intersections in Missouri

By
Praveen Edara, Ph.D., P.E., PTOE
Zhu Qing, Ph.D., P.E.
Henry Brown, P.E.
Carlos Sun, Ph.D., J.D., P.E.
Ho Jun Baek
University of Missouri

Prepared for
Missouri Department of Transportation

July 2024

Final Report

Copyright

Disclaimer

The opinions, findings, and conclusions expressed in this document are those of the investigators. They are not necessarily those of the Missouri Department of Transportation, U.S. Department of Transportation, or Federal Highway Administration. This information does not constitute a standard or specification.

Acknowledgments

The authors would like to thank the Missouri Department of Transportation (MoDOT) and the Missouri Center for Transportation Innovation (MCTI) for sponsoring this research. Special thanks are also extended to the Technical Advisory Committee for their guidance. Additionally, the authors appreciate the contributions of undergraduate research assistants Corey Valleroy, Velissia Perez, Mya Wood, Colin Kilcoin, and Scott McCool, who assisted with the data collection.

Table of Contents

List of Tables

List of Figures

List of Abbreviations and Acronyms

AADT	annual average daily traffic
AASHTO	American Association of State Highway and Transportation Officials
AIC	Akaike information criterion
CAD	computer-aided design
CG	comparison group
CMF	crash modification factor
CURE	cumulative residuals
EB	empirical Bayes
FI	fatal and injury
FDI	fatal and disabling injury
HSM	Highway Safety Manual
MAD	mean absolute deviation
MoDOT	Missouri Department of Transportation
R^2_{adj}	adjusted R-squared
RCI	reduced conflict intersection
RCUT	restricted crossing U-turn
SPF	safety performance function
St. E.	standard error
vpd	vehicle per day

ABSTRACT

The design of J-turn intersections has gained its prevalence in Missouri due to their demonstrated safety benefits. However, with the growing number of J-turns and the availability of more crash data, there is a renewed need to deepen the understanding of the safety performance of J-turns. This study presents a comprehensive safety evaluation of J-turn intersections, analyzing their effectiveness in reducing total and fatal & injury crashes using crash data from 47 J-turn intersections between 2005 and 2021. Employing a robust methodology including both comparison group and empirical Bayes analyses, this study assesses the impact of J-turns on crash reductions compared to traditional two-way stop-controlled intersections. Two methods were used because they had different tradeoffs such as data requirements, simplicity of implementation, and regression to the mean. The comparison group analysis revealed reductions of 74.6% in fatal and disabling injury crashes, 46.6% in fatal and injury crashes and 44.4% in total crashes. Similarly, the empirical Bayes analysis supported these safety improvements, showing reductions of 51.4% in fatal and injury crashes, 52.3% in fatal-and-injury excluding possible injury crashes, and 40.3% in total crashes. Furthermore, crash frequency models developed for Missouri's J-turn sites indicate that site characteristics such as loons, deceleration/acceleration lanes, and islands contribute to reduction in crashes. The study also includes detailed collision diagrams that outline crash locations and types at J-turn sites. The study findings provide insights and tools for MoDOT engineers as they consider J-turn design as a safety countermeasure at two-way stop-controlled intersections on rural highways.

EXECUTIVE SUMMARY

The Missouri Department of Transportation (MoDOT) has implemented J-turn intersections to improve road safety on rural highways since 2007. Traditional two-way stop-controlled intersections, especially those that allow direct crossing and left turns across multilane highways, present significant risks for severe crashes. J-turns, by design, mitigate these risks by directing vehicles to turn right and then perform a U-turn at a designated median opening. The primary objective of this study was to evaluate the safety performance of J-turn intersections in Missouri.

The research employs a robust methodological framework combining comparison group and empirical Bayes (EB) analyses, crash frequency modeling, and collision diagram analysis to provide a comprehensive evaluation. Data was collected from 47 J-turn intersections that have been installed across Missouri. The study period from 2005 to 2021 provided several years before and after the J-turn installations, allowing for a long-term steady analysis of crash data. In addition, data from 60 traditional two-way stop control intersection sites were also collected for comparison group analysis.

- Comparison Group Analysis

The comparison group (CG) analysis examined the data of 20 paired J-turns and traditional intersections. Altogether, there were a total of 395 crashes, including 17 fatal and disabling injury (FDI) crashes, recorded at the 20 J-turns in the study. The results showed that the crash modification factor (CMF) values for 72% of the J-turn sites were below 1.0, suggesting a decrease in total crashes, fatal and injury (FI) crashes, and FDI crashes after their installation. While the CMF exceeded 1.0 at five sites, these values were not statistically significant at the 95% confidence level. Overall, the CG results showed a reduction of 44.4% in total crashes, 46.6% in FI crashes, and 74.5% in FDI crashes at the 95% confidence level. The CG results demonstrate that converting from a two-way stop control to a J-turn significantly decreases the number of FI crashes, total crashes, and especially FDI crashes.

- Empirical Bayes Analysis

The empirical Bayes analysis examined the data of 32 J-turn intersections. Altogether, there were 682 crashes, including 167 FI crashes, recorded at the 32 J-turn in the study. The results showed that 85.9% of sites had a CMF value below 1.0. For FI and FI (KAB) crashes, although eight sites had CMF values greater than 1.0, none was statistically significant. For total crashes, 17 sites demonstrated a significant reduction at the 95% confidence level, but two sites experienced a significant increase. After reviewing the CMF calculations and crash data, the likely cause of the unexpected increase was identified as the lack of minor road AADT data, which could have resulted in inaccurate crash predictions. Overall, the EB analysis showed J-turns reduced FI crashes by 51.4%, FI (KAB) crashes by 52.3%, and total crashes by 40.3%.

- J-turn Crash Frequency Modeling

J-turn crash frequency modeling provided insights into how J-turn-design characteristics impact safety. Using data from 26 J-turns, which recorded a total of 412 crashes, including 131 FI crashes, regression models were developed to predict crash frequency. The results showed that design features like the presence of deceleration/acceleration lanes, loons, and islands had a positive impact on safety. The J-turn sites with left turn lanes on the major road experienced a higher number of crashes than sites without any left turn lanes. This finding was expected as left turn lanes were typically provided at sites with high overall traffic volume and left turning volumes.

- Collision Diagram Analysis

The collision diagram analysis helped identify crash types and locations within the J-turn area (as shown in Figure E.1), enhancing the understanding of how safety features can mitigate crash risk. The analysis showed a shift from right-angle and left-turn collisions at traditional intersections to sideswipe collisions at J-turns. Notably, most crashes occurred where minor road traffic merges onto highways, rather than at U-turn locations. The observed crash locations also suggest how J-turn designs, such as acceleration/deceleration lanes can effectively mitigate risks.

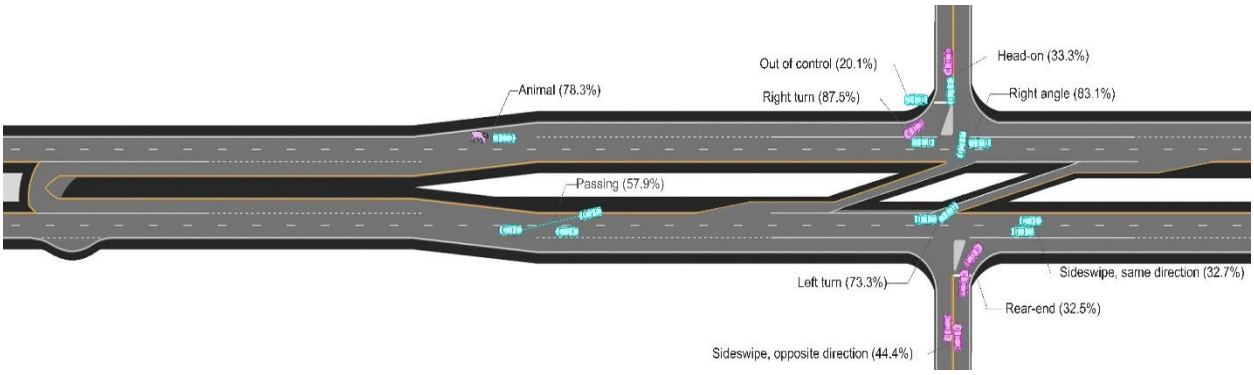

Figure E.1. Most frequent crash location for each type of crash.

In summary, the safety analysis of Missouri's J-turn installations provides robust evidence of a significant reduction in crashes. The CMFs and collision diagrams generated in this study can help MoDOT select sites and design criteria for future J-turn installations in the state.

1. INTRODUCTION

Minor road stop-controlled intersections on rural multilane highways are considered particularly higher risk prone to more severe crashes (Maze et al. 2010). A significant portion of these injury crashes are associated with turning movements with left turns across the highway, posing a risk of right-angle collisions. To mitigate this issue, the J-turn intersection, also known as a superstreet, restricted crossing U-turns (RCUTs), or reduced conflict intersections (RCIs), has been implemented. This design reroutes left turning and through traffic to make U-turns downstream, thereby avoiding direct crossings of the highway.

In Missouri, previous research has shown that J-turns have reduced total crashes by 35% and fatal and injury crashes by 54% (Edara et al. 2013), which has encouraged wider use of this intersection design. By 2022, Missouri had installed 47 J-turn intersections. However, the initial study was limited to only five J-turn intersections, suggesting a need for more comprehensive research to verify the safety benefits of J-turns throughout the state.

1.1 Project Objective

The project objective is to investigate the safety effectiveness of J-turn intersections in Missouri. The research methodology to meet the objectives includes a literature review, study design, data collection and analysis. The attainment of the project will lead MoDOT to a greater understanding of the safety benefits of J-turns and the effect of site characteristics (e.g., geometrics, traffic volume) on crash frequency and severity.

1.2 Project Overview

This report offers a comprehensive overview of the literature on the safety benefits of J-turn intersections and details the methodologies used in this analysis, including data collection, the comparison group (CG), and empirical Bayes (EB) methods for assessing safety benefits. Additionally, it outlines the techniques used for modeling J-turn crash frequency and conducting collision diagram analysis to evaluate site characteristics. The findings from these analyses are presented in the subsequent sections. The report concludes with a chapter summarizing the key research findings. Appendices provide a detailed summary of the J-turn data collected.

2. LITERATURE REVIEW

Previous research has shown the effectiveness of J-turn intersections in reducing traffic crashes through various analytical methods. Earlier studies frequently employed the CG and simple before-after (naïve) methods to evaluate the safety benefits of J-turns. For example, Lu et al. (2001) compared crash data from 125 J-turn intersections in Florida with 133 untreated intersections, identifying a 22.0% reduction in injury crashes and a 21.5% reduction in angle crashes, despite a 32.0% increase in sideswipe crashes, culminating in an overall crash rate reduction of 17.8% at a 95% confidence level.

Further employing the simple before-after method, Hochstein et al. (2009) analyzed four intersections in North Carolina and found total crash reductions ranging from 47.62% to 91.92%, with right-angle crash reductions between 91.67% and 100%. Similarly, Leuer and Fleming (2017) reported a 77% decrease in all severity right-angle crashes and a 100% elimination of fatal and serious injury right-angle crashes across eight J-turns in Minnesota using the simple before-after approach. Hummer and Rao (2017) observed CMFs of 0.85 for total crashes and 0.78 for injury crashes using a before-and-after comparison analysis with data from 11 signalized intersections across Alabama, North Carolina, Ohio, and Texas.

The EB method is another popular approach for investigating the impact of J-turns. Hummer et al. (2010) applied the EB method to 13 unsignalized J-turns in North Carolina and noted a 27.2% reduction in total crashes and an 85.9% reduction in angles and right-turn crashes. Inman and Haas (2012) performed an EB analysis and found a 44% reduction in total crashes and 9% reduction in fatal-and-injury crashes when analyzing nine RCUTs in Maryland. Edara et al. (2015) used EB to evaluate five unsignalized intersections in Missouri and reported a 54.4% reduction in total crashes, with substantial decreases across various severity levels, supporting the J-turns' safety benefits. Sun and Rahman (2019) extended this analysis to 10 J-turns in Louisiana (2 signalized, 8 unsignalized), finding a 31.1% reduction in total crashes, a 41.8% reduction in injury crashes, and a 100% reduction in fatal crashes when considering only the main intersection.

As summarized in Table 2-1, previous studies have shown varying CMF values for J-turns across among different states. In addition, the diverse characteristics of J-turn sites further impact their safety performance. For example, Sun and Rahman (2019) differentiated complete J-turns (including the U-turn areas) from partial J-turns, calculating separate CMFs of 0.87 and 0.89, respectively for total and injury crashes. Al-Omari et al. (2020) and Ulak et al. (2020) further analyzed signalized and unsignalized intersections, highlighting the influence of factors like speed limits, lane configurations, and intersection geometries on CMF values. Mishra and Pulugurtha (2022) categorized J-turn intersections by geographic characteristics and types, noting crash reductions ranging from 65% to 95% in various configurations. They also highlighted variations in crash reductions at rural and suburban signalized J-turns, showing only a slight decrease in total crashes at rural sites compared to more significant reductions at suburban locations.

While the research consistently supports the safety benefits of J-turns, previous research highlighted the variability of safety performance of J-turns, which can significantly depend on J-turn intersection configuration and other site characteristics. Therefore, there is a pressing need for further evaluation of the safety effectiveness of J-turns in Missouri. The evaluation should incorporate more sites and more up-to-date data, with the use of robust methodology to thoroughly assess their safety benefits.

Table 2-1. Summary of crash reductions and CMF values for J-turns from previous studies.

Description	State or Province	Crash Reduction	CMF Value	Quality Rating*	Reference
4 sites (2001-2006)	MD, NC	69.9% to 91.9% decrease in total crashes	Rural: 0.08 Suburban: 0.30	1	Hochstein et al. 2009
13 sites (1991-2010)	NC	46% decreased in total crashes	Total: 0.54	3	Hummer et al. 2010
4 sites (3 years)	NC, MD	30% decrease in annual crash rate	Rural:0.56	2	Inman and Haas 2012
5 sites (2-5 years)	MO	34.8% in overall crashes 53.7% in injury crashes	Total: 0.65 Injury: 0.46	4	Edara et al. 2015
11 sites (2002-2014)	AL, NC, OH, TX	4.53% in overall crashes	Total: 0.85 Injury: 0.78	3	Hummer and Rao 2017
10 sites (2008-2019)	LA	18.49% in overall crashes	4-leg: 0.80 3-leg: 1.07	4	Sun and Rahman 2019
225 sites	AL, GA, IL, IN, LA, MD, MI, MN, MS, MO, NC, OH, SC, TN, TX, WI	-	Total: 1-1.169 Injury: 0.955-1	4	Ulak et al. 2020
12 sites	MI, NC, OH	-	Total: 0.763 Injury: 0.567	2	Al-Omari et al. 2020

* Quality rating is a star rating system (ranging from 1 to 5) used by the CMF Clearinghouse to evaluate the quality of CMFs, where a 5 represents the highest level of reliability.

3. METHODOLOGY

This chapter is organized into five sections, each outlining a specific methodology aspect of the study: (1) the methodology for data collection, (2) the CG before-after method, (3) the EB before-after method, (4) procedures for modeling J-turn crash frequency, and (5) the methodology employed in the collision diagram analysis.

3.1 Data Collection

To examine the impact of J-turn site characteristics on traffic safety, a detailed analysis of J-turn sites was performed to gather both general and geometric data for this study.

3.2.1 General Data Collection

The general information of each site includes the number of lanes, speed limit, annual average daily traffic (AADT) on major and minor roads, the number of signs, and the number of access points. The data source for the general information includes design plans provided by MoDOT, MoDOT Crash Statistics Map, MoDOT Traffic Volume Maps and Google Earth Pro.

3.2.2 Geometric Data Collection

Geometric information encompasses data and measurements related to the layout of both highways and minor roads. For the highway, this includes the number of U-turns, through lanes, the presence of a loon, whether left turns from the highway to minor roads are permitted, and the existence of left-turn offsets. Figure 3.1 shows an example of how geometric information is collected from an aerial image of US 65 from Google Earth Pro.

Figure 3.1. Highway geometric data for MO 13 & Route U and Route Y, Bolivar, MO.

For minor roads, the following details are collected using Google Earth Pro's aerial imagery: the number of lanes on the minor road approach, the presence of a deceleration lane for right turns from the highway, the presence of an acceleration lane for right turns from the minor road, the existence of a splitter island on the minor approach, the presence of a painted island on the minor approach, the use of flexible delineators to separate acceleration lanes from through lanes, the presence of median deceleration lanes, and the presence of median acceleration lanes. Figure 3.2 shows how the geometric information is gathered from an aerial image of MO 215.

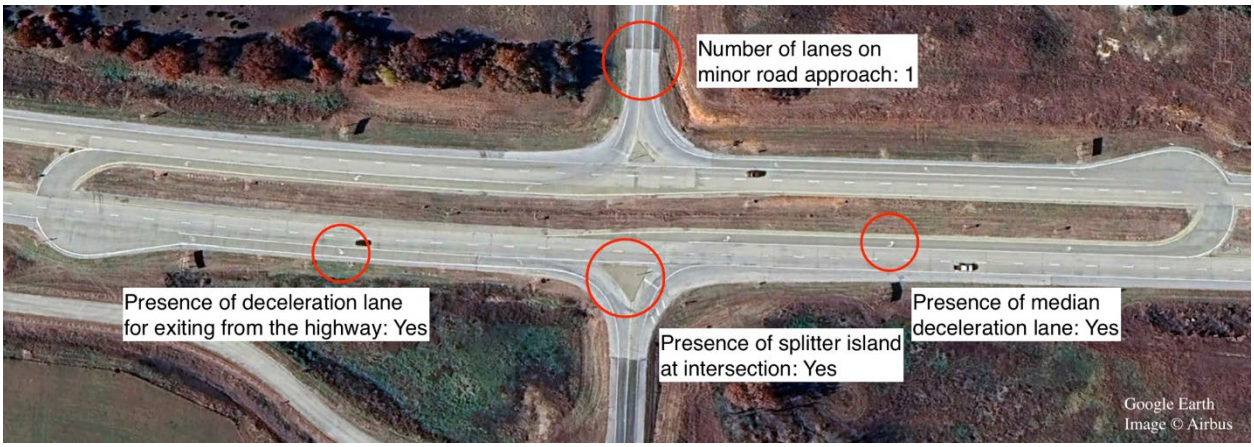

Figure 3.2. Minor road geometric data for US 65 & MO 215, Fair Grove, MO.

In addition to recording presence and quantity information, data were also derived from design plans or by using measurement tools available in Google Earth Pro. Key metrics recorded included the median width, the distance from the minor road to the downstream U-turn, the skew angle of the intersection, the horizontal curve radius at the highway intersection, and the vertical grade of the highway at the intersection. The "Ruler" tool in Google Earth was utilized to measure width, distance, and skew angle. This tool provides the length and direction of a line drawn on the map. By comparing the headings of the major and minor roads, the skew angle of the intersection is calculated. Figure 3.3 demonstrates how these measurements were taken for US 65 & MO 215. According to these measurements, the distance from the minor road to the downstream U-turn is 586.36 feet, and the skew angle is 87.71 degrees (271.47 - 183.76 = 87.71).

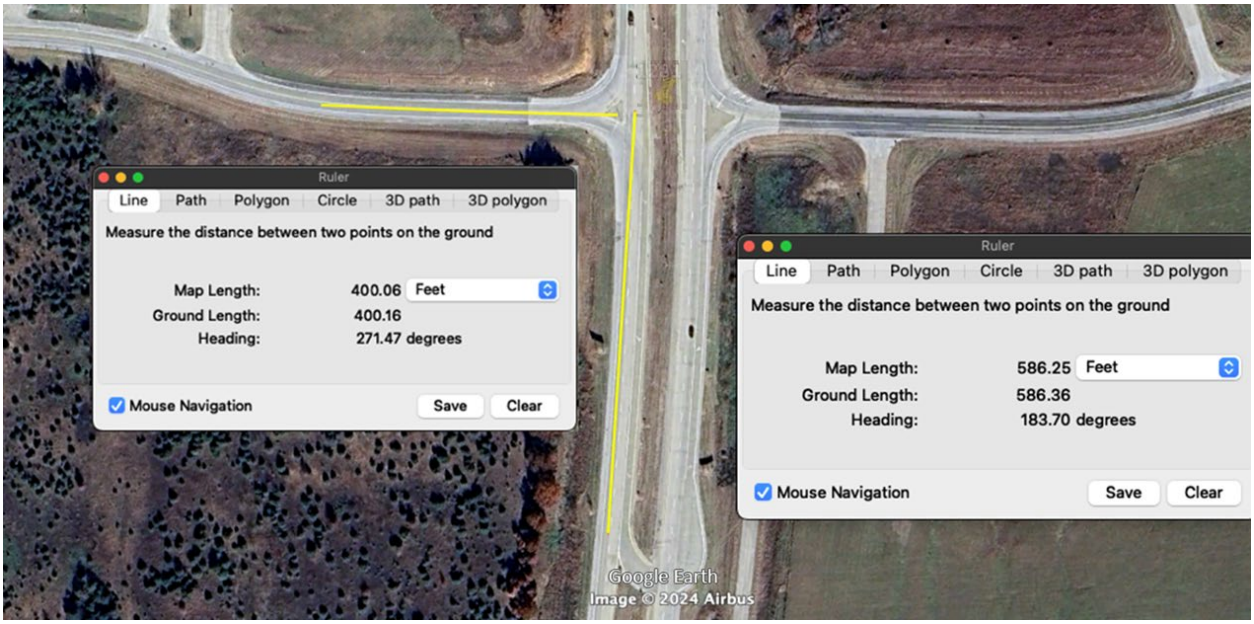

Figure 3.3. Measurements of US 65 & MO 215, Fair Grove, MO.

3.2 Comparison Group Method

The CG method identifies a group of untreated facilities, similar to the treated facilities before construction of the J-turn intersections, to estimate the measure of how safety would have changed for the treatment group. It is assumed that different factors influence safety in the same manner for the treatment and sites in the control group during the before and after periods (Hauer 1997).

Each comparison site needs to be carefully selected to resemble the traffic, geometry, and crash frequency of the treatment site before the J-turn implementation. In this study, a comparison site was selected from the same MoDOT district as the J-turn site to ensure a similar driving population. The suitability of the CG analysis was verified with the sample odds ratio test (Equation 3-1) (Hauer 1997; Gross, Persaud, and Lyon 2010).

$$Sample\ odds\ ratio = \frac{\frac{Treatment_i \cdot Comparison_{i+1}}{Treatment_{i+1} \cdot Comparison_i}}{1 + \frac{1}{Treatment_{i+1}} + \frac{1}{Comparison_i}} \qquad \text{(Equation 3-1)}$$

Where,
Treatment $_i$ = total crashes for the treatment group in year i.
Treatment $_{i+1}$ = total crashes for the treatment group in year i+1.
Comparison $_i$ = total crashes for the comparison group in year i.
Comparison $_{i+1}$ = total crashes for the comparison group in year i+1.

For each before-and-after pair before the implementation of the treatment, sample odds ratios are calculated. The sequence of these sample odds ratios allows for the calculation of the sample mean and standard error (St. E.). If the sample mean closely approximates 1.0, it indicates that the selected reference group is appropriately matched.

After the reference group is selected, the comparison ratio ($N_{observed, C, A}/N_{observed, C, B}$) is calculated to estimate the change in the absence of treatment. The expected number of crashes for the treatment group that would have occurred in the after period without treatment is estimated from Equation 3-2 (Gross, Persaud, and Lyon 2010).

$$N_{expected,T,A} = N_{observed,T,B}\left(\frac{N_{observed,C,A}}{N_{observed,C,B}}\right) \qquad \text{(Equation 3-2)}$$

Where,
$N_{expected, T, A}$ = the expected number of crashes in the after period for the treatment group.
$N_{observed, T, A}$ = the observed number of crashes in the after period for the treatment group.
$N_{observed, C, A}$ = the observed number of crashes in the after period in the comparison group.
$N_{observed, C, B}$ = the observed number of crashes in the before period in the comparison group.

The variance of $N_{observed,\,T,\,B}$ is estimated approximately from Equation 3-3. This estimate serves as an approximation, as it assumes the existence of yearly trends in perfectly identical pairs, a scenario that is virtually unattainable. However, the difference between the precise estimation and the approximation is typically minor (Hauer 1997).

$$Var\left(N_{expected,T,A}\right) = N_{expected,T,A}^{2}\left(\frac{1}{N_{observed,T,B}} + \frac{1}{N_{observed,C,B}} + \frac{1}{N_{observed,C,A}}\right) \quad \text{(Equation 3-3)}$$

The CMF and its variance are estimated from Equation 3-4 and 3-5 (Gross, Persaud, and Lyon 2010).

$$CMF = \left(\frac{N_{observed,\,T,\,A}}{N_{expected,\,T,\,A}}\right)/\left(1 + \left(\frac{Var\left(N_{expected,\,T,\,A}\right)}{N_{expected,\,T,\,A}^{2}}\right)\right. \quad \text{(Equation 3-4)}$$

$$Variance(CMF) = \frac{CMF^{2}\left[\left(1/N_{observed,\,T,\,A}\right) + \left(\frac{Var\left(N_{expected,\,T,\,A}\right)}{N_{expected,\,T,\,A}^{2}}\right)\right]}{\left[1 + \frac{Var\left(N_{expected,\,T,\,A}\right)}{N_{expected,\,T,\,A}^{2}}\right]^{2}} \quad \text{(Equation 3-5)}$$

3.3 Empirical Bayes Before-After Method

Similar to the CG method, the EB method compares the sum of estimates of $N_{expected,\,T,\,A}$ for all treated sites with the number of crashes actually occurred after treatment (Gross, Persaud, and Lyon 2010). However, the EB method provides a more accurate estimation of crashes that would have occurred at an individual treated site in the after period had a treatment not been implemented, as it correctly accounts for observed changes in crash frequencies before and after a treatment that may be due to regression-to-the-mean. EB is more accurate than CG but is more laborious to implement.

The EB estimate of the expected number of crashes without treatment, N expected, T, A, is computed from Equation 3-6 (Gross, Persaud, and Lyon 2010).

$$N_{expected,T,B} = SPF\ weight \times N_{predicted,T,B} + (1 - SPF\ weight) \times N_{observed,T,B} \quad \text{(Equation 3-6)}$$

Where,

$N_{expected,\,T,\,B}$ = the expected number of crashes in the before period for the treatment group

$N_{predicted,\,T,\,B}$ = the predicted number of crashes estimated by the SPF in the before period.

$N_{observed,\,T,\,B}$ = the observed number of crashes in the before period for the treatment group.

The safety performance function (SPF) weight is derived using the overdispersion parameter (k) from the SPF and the number of years of crash data in the period before treatment from Equation 3-7 (AASHTO 2010). The SPF weight is reduced if more years of crash data are used.

$$SPF\ weight = \frac{1}{1 + k \times \left(\sum_{years} N_{predicted,T,B}\right)} \quad \text{(Equation 3-7)}$$

The predicted number of crashes, $N_{predicted}$, is estimated using the crash prediction methodology in the Highway Safety Manual (HSM) (AASHTO 2010). As shown in Equation 3-8, the predictions also incorporate the corresponding CMFs for each site with the before period characteristics and calibration factor for local conditions.

$$N_{predicted} = N_{SPF} \times C_i \times \left(CMF_1 \times CMF_2 \times \cdots \times CMF_j\right) \quad \text{(Equation 3-8)}$$

Where,
$N_{predicted}$ = the predicted number of crashes.
N_{SPF} = the predicted number of crashes under the baseline conditions by the SPF.
C_i = calibration factor for local conditions.
CMF_j = crash modification factors specific to site, geometric design, and traffic control features.

The predicted crash numbers for J-turn intersections utilize the prediction model for intersections on rural multilane highways outlined in the HSM (AASHTO 2010). The prediction model is used to estimate the number of crashes for the before and after periods (Equation 3-9).

$$N_{SPF} = \exp\left[\ (a + b \times \ln\left(AADT_{major}\right) + c \times \ln(AADT_{minor})\right] \quad \text{(Equation 3-9)}$$

Where,
$AADT_{major}$ = AADT for major-road approaches.
$AADT_{minor}$ = AADT for minor-road approaches.
a, b, c = regression coefficients.

The regression coefficients vary depending on the type of intersection and the type of severity. Table 3-1 shows the coefficients for the different types as provided in the HSM (AASHTO 2010).

Table 3-1. SPF coefficients for three-leg and four-leg intersections with minor-road stop control for total, fatal-and-injury, and fatal-and-injury excluding possible injury (KAB) crashes (AASHTO 2010).

Intersection type/severity level	a	b	c	Overdispersion parameter (fixed k)
4-leg intersection, total	-10.008	0.848	0.448	0.494
4-leg intersection, FI	-11.554	0.888	0.525	0.742
4-leg intersection, FI (KAB)	-10.734	0.828	0.412	0.655
3-leg intersection, total	-12.526	1.204	0.236	0.460
3-leg intersection, FI	-12.664	1.107	0.272	0.569
3-leg intersection, FI (KAB)	-11.989	1.013	0.228	0.566

Regarding the CMF specific to site characteristics, geometric design, and traffic control features, the value of CMF j is based on the recommendations provided in Chapter 14 of the HSM (AASHTO 2010). The CMF values used in the study are detailed in Table 3-2.

Table 3-2. CMF for intersection skew angle, left-turn lane, and right-turn lane from the HSM (AASHTO 2010).

CMF	3-leg intersection, total	3-leg intersection, FI and FI (KAB)	4-leg intersection, total	4-leg intersection, FI and FI (KAB)
Skew	(0.016×skew)/(0.98+0.16×skew) + 1	(0.017×skew)/(0.52+0.17×skew) + 1	(0.053×skew)/(1.43+0.53×skew) + 1	(0.048×skew)/(0.72+0.48×skew) + 1
Left-turn Lane	0.56	0.45	0.72 (one approach) 0.52 (two approaches)	0.65 (one approach) 0.42 (two approaches)
Right-turn Lane	0.86	0.77	0.86 (one approach) 0.74 (two approaches)	0.77 (one approach) 0.59 (two approaches)

The local calibration factors for Missouri were updated in 2018 (Sun et al. 2018). According to the recalibration, the calibration factors for total crashes were set as 0.95 for three-leg intersections and 0.65 for four-leg intersections. Since there were no available calibration factors for FI and FI (KAB), a default value of 1.0 was used.

The adjusted value of the EB estimate, N expected, T, A, is the expected number of crashes in the after period without treatment and is calculated from Equation 3-10 (Gross, Persaud, and Lyon 2010).

$$N_{expected,T,A} = N_{expected,T,B}(N_{predicted,T,A}/N_{predicted,T,B}) \quad \text{(Equation 3-10)}$$

Where,
$N_{expected, T, A}$ = the unadjusted empirical Bayes estimate.
$N_{predicted, T, A}$ = the predicted number of crashes estimated by the SPF in the after period.

The variance of $N_{expected, T, A}$ is estimated from $N_{expected, T, A}$, the before and after SPF estimates, and the SPF weight, from Equation 3-11 (Gross, Persaud, and Lyon 2010).

$$Var(N_{expected, T, A}) = N_{expected, T, A}\left(\frac{N_{predicted, T,A}}{N_{predicted, T, B}}\right)(1 - SPF_{weight}) \qquad \text{(Equation 3-11)}$$

The CMF and its variance are estimated same as the CG method from Equation 3-4 and 3-5.

3.4 J-turn Crash Frequency Modeling

J-turn crash frequency modeling is a statistical approach to estimate the number of crashes that are likely to occur at J-turn intersections using existing traffic and crash data. This modeling approach also allows for an assessment of how different J-turn design features, such as the presence of acceleration or deceleration lanes, loons, and island, affect intersection safety. These insights cannot be obtained through the aforementioned CG and EB methods.

Crash frequency modeling uses a range of analytical methods to determine the optimal functional form for the relationship between crash counts and independent variables. Much of the analysis is conducted using R, an open-source programming language. To evaluate and compare the quality of the frequency models, several measures are employed, including the overdispersion parameter (k), adjusted R-Square (R^2_{adj}), mean absolute deviation (MAD), Akaike information criterion (AIC), and cumulative residual (CURE) plots.

(1) Overdispersion parameter

For most of the crash data, the variance is larger than the mean of crash frequency. This phenomenon is called overdispersion. Negative binomial regression allows the variance to differ from the mean by introducing an overdispersion parameter, k. The smaller value of k is preferred as it indicates the model is with less variation and the distribution is closer to a Poisson model.

(2) Adjusted R-Squared

R^2_{adj} is a frequently used measure indicating the proportion of variance in the dependent variable that is predictable from the independent variables. R^2_{adj} is particularly useful in multiple regression models and for model selection. The value of R^2_{adj} ranges from 0 to 1, where higher values indicate a better fit.

(3) Mean absolute deviation

The mean absolute deviation (MAD) is a measure of variability that indicates the average distance between observation values and predicted mean values over the number of observations. Smaller values are preferred to larger values.

(4) Akaike information criterion

The AIC describes the trade-off between bias and variances. The AIC is computed as Equation 3-12 (Hauer 2015). A lower value of AIC is preferred.

$$AIC = 2k - 2LL \qquad \text{(Equation 3-12)}$$

Where,
k = the number of estimated parameters in the model.
LL = the maximized value of the likelihood function for the model.

(5) Cumulative residual (CURE) plots

The method of CURE plots is presented by Hauer (2015). In the CURE plots, the cumulative residuals are plotted in increasing order for each covariate separately. The graph is able to show how well the model fits the observations for each individual variable. One difference between CURE and the previous four performance measures is that CURE is not a single statistic but a plot of the performance of the model across the range of values for the independent variable. Thus, it is able to diagnose if the model is performing well across the whole range of values.

Multiple performance measures are used because they reveal different aspects of model performance. Further details are provided in the Art of Regression Modeling in Road Safety (Hauer 1997), and the Safety Performance Function Development Guide: Developing Jurisdiction-Specific SPFs (Srinivasan and Bauer 2013).

3.5 Collision Diagram Analysis

Collision diagram serves as a visual analysis tool to analyze and understand the location, type, contributing factors, and distribution of crashes. It offers valuable insights into impacts of J-turn geometry and operational characteristics on the observed type of crashes observed.

In this study, a three-step methodology was employed to create collision diagrams, focusing on crash type, location, and distribution. First, as shown in Figure 3.4, a diagram of a J-turn intersection is generated. The intersection diagram integrated various geometric features which are typically found at J-turn intersections, such as acceleration and deceleration lanes for both mainline and minor-road traffic, left turn lanes for mainline traffic, loons, and separate islands. It will be used as the foundational diagram to which crash data are subsequently added.

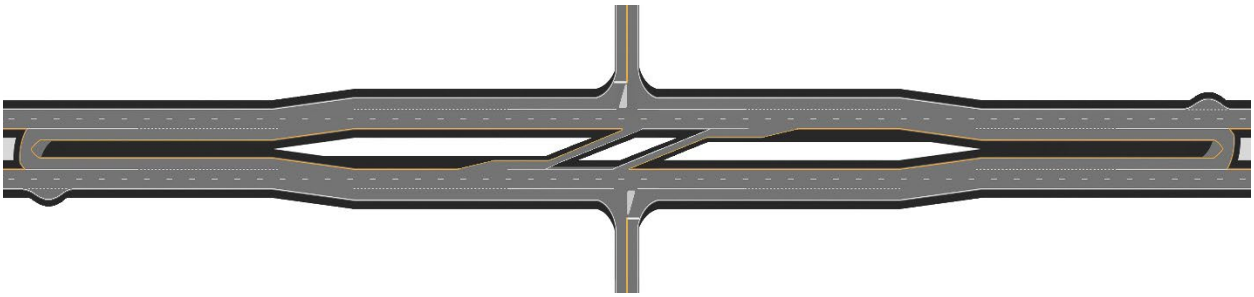

Figure 3.4. J-turn collision foundational diagram.

Secondly, crash reports were reviewed on a case-by-case basis and the crash details summarized on the foundational diagram using computer-aided design (CAD) software. The advantages of using CAD include location accuracy, and the storage of detailed information for future analysis such as crash type and location.

Identifying the exact location of a crash can be challenging, especially if it involves multiple vehicles and objects. For example, a vehicle may collide with another vehicle's side due to swerving to avoid debris on the road. Therefore, the crash location is recorded as a point in CAD solely based on the point of impact as stated in the crash report (Figure 3.5), which marks the location of the initial impact.

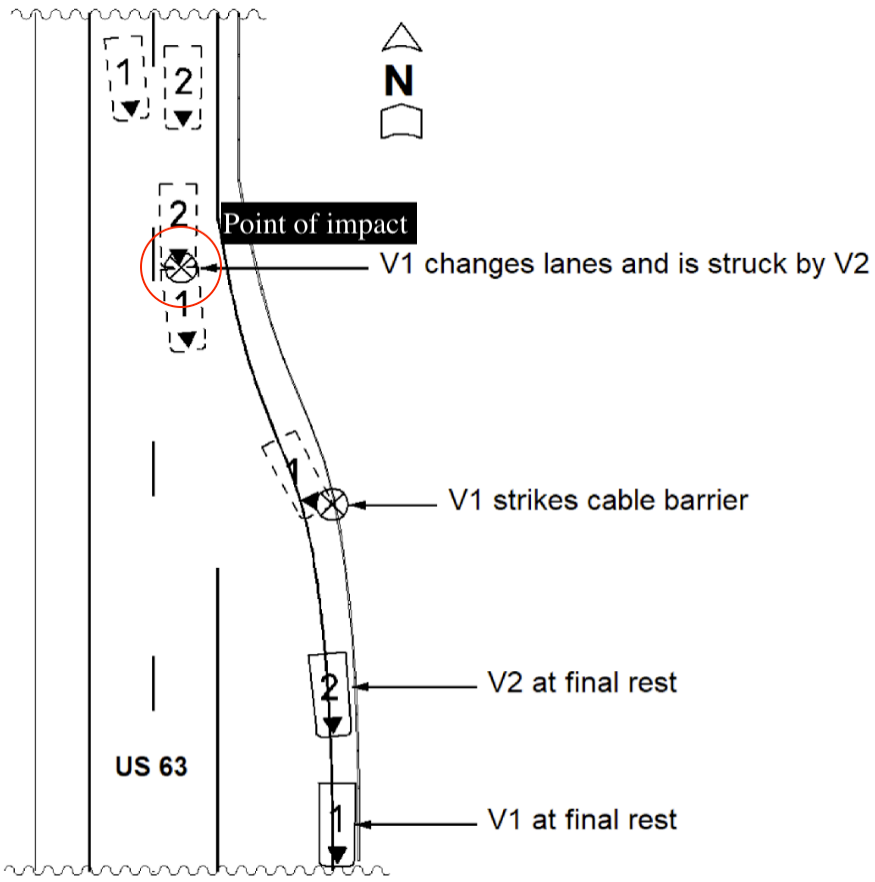

Figure 3.5. Example - point of impact as documented in crash report.

The crash type is coded and saved with the point of location by layers. The crashes of the same type share a layer to facilitate easier filtering and analysis in the future. The crash types include head-on crashes, animal collisions, left turns, out-of-control incidents, passing, rear-end collisions, right-angle crashes, right turns, sideswipes in the same direction, and sideswipes in the opposite direction. Definitions for each crash type are summarized in Table 3-3.

Table 3-3. Crash type and definition.

#	Crash Type	Definition
1	Head-on	The front ends of two vehicles collide with they are traveling in opposite direction.
2	Animal	Crashes between vehicles and wildlife when the animal is crossing a road.
3	Left turns	A vehicle attempting to make a left turn collides with an oncoming vehicle.
4	Out-of-control	A driver loses control of the vehicle.
5	Passing	A vehicle collides with other objects/vehicles while attempting to overtake another vehicle.
6	Rear-end	A vehicle collides with the rear of another vehicle.
7	Right-angle	A vehicle collides with the side of another vehicle, resulting in a right angle between the two vehicles
8	Right turns	A vehicle attempting to make a right turn collides with an oncoming vehicle.
9	Sideswipes in the same direction	A collision between the sides of both vehicles when both vehicles are traveling in the same direction.
10	Sideswipes in the opposite direction	A collision between the sides of both vehicles when the vehicles are traveling in opposite directions.

Third, the filtered crashes are analyzed and sorted by type and location. The frequency of each category is then displayed using collision diagrams. These diagrams are utilized to identify crash patterns and to analyze trends and common factors that contribute to accidents at J-turn intersections.

4. SAFETY EVALUATION RESULTS

4.1 Data Description

As of 2024, there are a total of 47 J-turn intersections on four-lane highways built in Missouri. The geometric characteristics of all J-turn intersections were collected are listed in Appendix A. However, 14 sites were excluded from the list because these sites were installed after 2020 and historical crash data was not available. Additionally, one site was excluded because it became a 3-leg intersection from 4-leg intersection after the J-turn installation. Two sites were excluded because left turns from the minor road to join highway are still allowed. Therefore, this study included 30 intersections in Missouri. All 30 sites were unsignalized intersections of rural two-lane highway with minor roads intersecting. Among these 30 sites, 28 sites were 4-leg intersections, and 2 sites were 3-leg intersections. To mitigate the novelty effect associated with the introduction of J-turns, crash data from the year of the J-turn installation and the year following installation were excluded from analysis.

The crash reports for these sites from 2005 to 2021 (17 years) were reviewed. 2,781 crashes occurred before the installation of the J-turn, and 721 crashes occurred after the installation of J-turns. All the crashes after the installation were categorized using the KABCO injury classification scale, 1.2% fatal (K), 1.9% disabling (A), 2.5% evident injury (B), 18.9% possible (C), and 75.5% property damage only (O). The safety evaluation investigates the safety effects of J-turns on different types of crashes. Total crashes include all severity levels (KABCO). Fatal and disabling injury (FDI) crashes include fatal and disabling injuries (KA). Fatal and injury (FI) crashes include fatal, disabling, evident, and possible injuries (KABC). FI (KAB) crashes, excluding possible injury crashes, include only fatal, disabling, and evident injuries.

4.2 Comparison Group Method

4.2.1 Data Description

The HSM advises using at least 10 to 20 sites for conducting a safety evaluation. Specifically, for the CG method, it suggests a minimum of 650 aggregated crashes at comparable sites. In this study of J-turns, 20 paired sites were selected based on the availability of crash data and the outcomes of sample odds ratio results, with a total of 839 crashes recorded at these sites. As shown in Table 4-1, the sample odds ratio means of pared sites are near to 1.0 and are within the 95% confidence interval indicating that the comparison group is appropriate for the safety evaluation. To mitigate the regression-to-the-mean effects and not to over-estimate the effect of J-turns, particularly since the J-turns were usually installed at high crash count locations, recently converted J-turn sites were also included in comparison sites. For example, the comparison site for A6 (US 160 & Route 123, Springfield, MO) was converted to J-turns in 2020, and its crash data as a traditional intersection from 2005 to 2019 were used in the before and after analysis.

Due to the varying installation times of the J-turns, the before and after periods differed for each location. The before and after periods for each site are listed in Table 4-1, with an average before period of 8.25 years and an after period of 5.8 years.

Table 4-1. Results of the sample odds ratio for paired J-turn and comparison sites.

#	J-turn site	Comparison site	Sample odds ratio	95% confidence interval	Before period (years)	After period (years)
A1	US 54 and Route E, Jefferson City, MO	US 54 & Midway Road, Osage Beach, MO	1.004	0.245 – 1.763	7	8
A2	US 54 & Honey Creek Road, Jefferson City, MO	US 54 & Allen Road, Eldon, MO	0.989	0.368 – 1.611	7	8
A3	MO 30 & Osage Executive Drive, Byrnes Mill, MO	MO 30 & Scotsdale Boulevard, Scotsdale, MO	1.017	0.668 – 1.366	7	5
A4	US 65 & Rochester Road, Ridgedale, MO	US 65 & Route A and Route BB, Saddlebrooke, MO	0.805	-0.236 – 1.847	7	8
A5	US 63 & Route AB, Columbia, MO	US 63 & Angel Lane, Minor Hill Road, Ashland, MO	0.905	0.620 – 1.191	7	7
A6	US 65 & Red Top Road and Route EE, Buffalo, MO	US 160 & Route 123, Springfield, MO	1.046	-0.553 – 2.645	4	9
A7	US 65 & MO 215, Fair Grove, MO	US 160 & Route 123, Springfield, MO	0.795	0.544 – 1.046	4	9
A8	US 65 & Red Top Road and Route AA, Fair Grove, MO	US 60 & Business US 60, Rogersville, MO	1.031	-0.495 – 2.557	4	9
A9	MO 13 & Northeast Old Highway 13, Osceola, MO	MO 13 & 100 Rd, Collins, MO	1.086	0.078 – 2.094	3	12
A10	US 65 & MO 38, Buffalo, MO	US 160 & Route 123, Springfield, MO	1.024	-0.596 – 2.644	4	9
A11	US 63 & Hinton Road and Calvert Hill Road, Columbia, MO	US 54 & Route AA and Old Highway 54, Eugene, MO	0.937	0.359 – 1.515	9	6
A12	US 63 & Peterson Lane, Ashland, MO	US 63 & East New Salem Lane, Ashland, MO	0.875	0.412 – 1.339	9	5
A13	US 50 & MO 58, Centerview, MO	US 50 & Route 127, La Monte, MO	1.057	0.275 – 1.840	9	6
A14	US 63 & Main Street and Route M, Atlanta, MO	US 61 & Route A, New London, MO	1.081	0.056 – 2.107	9	4
A15	US 63 & Route P, Route B, Clark, MO	US 61 & Route A, New London, MO	0.803	0.454 – 1.152	9	4
A16	US 50 & MO 131, Holden, MO	US 50 & Northwest State Highway W, Kingsville, MO	1.022	0.584 – 1.460	12	1

#	J-turn site	Comparison site	Sample odds ratio	95% confidence interval	Before period (years)	After period (years)
A17	US 67 & New Perrine Road, Farmington, MO	US 67 & Route H, Farmington, MO	0.999	0.412 – 1.586	13	2
A18	US 50 & S Buckner Tarsney Road, Lone Jack, MO	US 50 & Route 127, La Monte, MO	1.195	0.475 – 1.915	13	2
A19	US 54 & Route A, Linn Creek, MO	US 54 & Allen Road, Eldon, MO	1.121	0.535 – 1.707	14	1
A20	US 54 & Old US 54, Osage Beach, MO	US 54 & Route FF, Eldon, MO	1.024	-0.286 – 2.335	14	1

In this CG study, certain J-turn locations were paired with a single comparison site using a yoked comparison approach. This pairing strategy was not based solely on similarities in geometric features and traffic volumes. Instead, it was largely driven by the widespread adoption of J-turns along particular corridors. For example, in the MoDOT Southwest District, five intersections on MO 13 were converted into J-turns in 2019. As a result, the yoked comparison primarily concentrated on corridors where multiple J-turns have been implemented together.

4.2.2 Results

The observed and expected total crashes, as well as FI and FDI crashes for each J-turn site, are presented in Table 4-2. The variability in crash numbers across different J-turns is largely attributed to some sites having been operational for longer periods than others. The CMF values are calculated using Equation 3-4, and the St. E. is computed as the square root of the CMF's variance. If the value of CMF is less than 1.0, it means that the J-turn had a positive safety benefit and helped to reduce the number of crashes.

The CMF values for most J-turns were below 1.0, suggesting a decrease in total, FI and FDI crashes after their installation. Half of the sites had FI crash reductions of over 50%, including seven with over 70%. In two sites, the CMF exceeded 1.0 and in two sites the FI CMF exceeded 1.0. Specifically, sites A12 and A18 exhibited greater than 1.0 CMF value for FI crashes, while sites A4 and A18 showed an upward trend in total crashes. However, the CMF values from all sites that had CMF greater than 1.0 were not statistically significant at the 95% confidence level. In other words, the data did not show a statistically significant change for the expected number of crashes at those sites. Additionally, due to the scarcity of FDI crashes, nine comparison sites did not have any FDI crashes during the study period and therefore CMF values could not be calculated for the paired J-turn sites.

The cumulative totals of crashes at all the selected J-turn sites are listed in the final row of the table. Altogether, there were a total of 395 crashes, including 161 FI crashes, recorded at the 20 J-turns in the study. Overall, the CG results showed a reduction of 44.4% in total crashes, 46.6% in FI crashes, and 74.5% in FDI crashes, at the 95% confidence level. The CG results show that a

conversion from a two-way stop control to J-turn decreases significantly the number of FI crashes and the total number of crashes, especially the number of FDI crashes.

Table 4-2. Results of the control group analysis.

#	Total crash observed after	Expected value after	CMF	St. E.	FI crash observed after	Expected value after	CMF	St. E.	FDI crash observed after	Expected value after	CMF	St. E.
A1	26	39.240	0.583*	0.215	12	15.380	0.628*	0.288	2	2.500	0.296	0.163
A2	25	38.330	0.603	0.194	6	24.550	0.201	0.102	0	12.000	0.000	-
A3	25	94.790	0.241	0.081	6	20.000	0.247	0.126	0	7.500	0.000	-
A4	33	27.000	1.058*	0.394	10	17.780	0.442	0.212	2	4.000	0.267	0.167
A5	28	79.570	0.342	0.085	10	15.970	0.558*	0.234	4	6.000	0.211	0.103
A6	8	31.000	0.196	0.099	0	2.500	-	-	0	-	-	-
A7	14	44.290	0.248	0.115	4	2.500	0.681*	0.367	0	-	-	-
A8	22	27.810	0.708*	0.256	7	6.190	0.793*	0.420	0	1.000	0.000	-
A9	37	42.000	0.658	0.297	11	27.000	0.229	0.120	2	2.500	0.296	0.163
A10	8	53.140	0.120	0.059	7	7.500	0.554*	0.299	2	-	-	-
A11	42	108.460	0.335	0.123	10	25.600	0.264	0.136	0	0.000	-	-
A12	34	35.890	0.838*	0.296	7	2.400	1.636*	0.883	2	0.000	-	-
A13	19	62.320	0.282	0.096	8	26.130	0.261	0.121	0	6.000	0.000	-
A14	6	28.540	0.193	0.090	1	14.250	0.059	0.054	1	7.333	0.100	0.085
A15	16	44.970	0.330	0.115	6	16.500	0.305	0.153	0	8.000	-	-
A16	10	16.610	0.560	0.218	2	2.538	0.573*	0.390	0	0.000	-	-
A17	13	13.670	0.880*	0.324	2	3.820	0.434*	0.302	1	0.400	1.064*	0.694
A18	19	12.940	1.281*	0.499	7	5.000	1.113*	0.560	1	0.000	-	-
A19	9	10.420	0.730*	0.335	1	2.190	0.221	0.153	0	0.000	-	-
A20	1	1.350	0.594*	0.533	0	0.400	-	-	0	0.000	-	-
Total	395	707.130	0.556	0.044	116	215.020	0.534	0.074	17	63.818	0.255	0.079

* Not significant at the 95% confidence level.

4.3 Empirical Bayes Before-After Method

4.3.1 Data Description

Out of 47 J-turn intersections in Missouri, 32 were appropriated for the EB before-and-after analysis using crash data spanning from 2005 to 2021. Of the 15 intersections not included, 14 J-turns were installed in 2020 or later and lacked sufficient crash data for reliable estimation. The intersection at US 63 and Old Millers Rd in Columbia, was also excluded from the evaluation due to its confounding effect, as it changed from a four-leg to a three-leg intersection.

The 32 J-turns locations are detailed in Table 4-3, including cross street names, number of intersection legs, major and minor AADT, installment year and before/after periods. Table 4-3 shows there were only three 3-leg intersections. The average maximum major road AADT was 20,876, and the average maximum minor road AADT was 2,337. There were no minor road AADT values for ten of the sites. The average year of installment was 2015.

Table 4-3. Selected J-turn intersections for the empirical Bayes analysis.

#	Location	Type	Major-approach AADT (vpd)	Minor-approach AADT (vpd)	Installment year	Before period (years)	After period (years)
B1	Route M and Old Lemay Ferry Connector, Barnhart, MO	3-leg	8,891 - 11,473	n/a	2007	2	13
B2	US 54 and Route E, Jefferson City, MO	4-leg	13,109 - 18,122	636-1910	2012	7	7
B3	US 54 & Honey Creek Road, Jefferson City, MO	4-leg	14,873 - 21,931	974-1085	2012	7	8
B4	US 54 & Route CC, Jefferson City, MO	3-leg	14,879 - 35,043	n/a	2012	7	8
B5	US 54 & Buffalo Road, Heritage Highway, Jefferson City, MO	4-leg	14,873 - 21,931	810-934	2012	7	8
B6	MO 30 & Osage Executive Drive, Byrnes Mill, MO	4-leg	22,352 - 33,580	2597-2735	2012	7	8
B7	US 65 & Rochester Road, Ridgedale, MO	4-leg	11,181 - 19,355	n/a	2012	7	8
B8	US 63 & Route AB, Columbia, MO	4-leg	23,292 - 33,697	n/a	2012	7	8
B9	US 65 & Red Top Road and Route EE, Buffalo, MO	4-leg	5,852 - 10,020	690-1194	2009	4	11
B10	US 65 & MO 215, Fair Grove, MO	4-leg	6,898 - 8,430	1090-2597	2009	4	11
B11	US 65 & Red Top Road and Route AA, Fair Grove, MO	4-leg	7,716 - 11,810	1336-2027	2009	4	11

#	Location	Type	Major-approach AADT (vpd)	Minor-approach AADT (vpd)	Installment year	Before period (years)	After period (years)
B12	MO 13 & Northeast Old Highway 13, Osceola, MO	4-leg	9,434 - 14,335	n/a	2008	3	12
B13	US 65 & MO 38, Buffalo, MO	4-leg	5,852 - 8,430	1570-2364	2009	4	13
B14	US 63 & Hinton Road and Calvert Hill Road, Columbia, MO	4-leg	13,855 - 21,693	n/a	2014	9	6
B15	US 63 & Peterson Lane, Ashland, MO	4-leg	24,617 - 30,918	n/a	2014	9	6
B16	US 50 & MO 58, Centerview, MO	4-leg	12,488 - 17,601	2821-3765	2014	9	6
B17	US 63 & Main Street and Route M, Atlanta, MO	4-leg	5,609 - 6,865	278-887	2014	9	6
B18	US 63 & Route P, Route B, Clark, MO	4-leg	11,817 - 16,471	848-1090	2014	9	6
B19	US 50 & MO 131, Holden, MO	4-leg	12,624 - 18,110	2843-3401	2017	12	3
B20	US 67 & New Perrine Road, Farmington, MO	4-leg	10,409 - 16,123	2705-2863	2018	13	2
B21	MO 13 & Route Y and Route U, Bolivar, MO	4-leg	15,695 - 20,635	1324-2310	2018	13	2
B22	US 50 & S Buckner Tarsney Road, Lone Jack, MO	3-leg	17,296 - 27,842	n/a	2018	13	2
B23	MO 13 & Calvird Drive, Clinton, MO	4-leg	11,583 - 13,081	1980-6250	2019	14	1
B24	US 54 & Route A, Linn Creek, MO	4-leg	20,483 - 33,755	1300-3048	2019	14	1
B25	MO 13 & MO 123, Humansville, MO	4-leg	7,522 - 10,383	1184-2145	2019	14	1
B26	US 54 & Old US 54, Osage Beach, MO	4-leg	9,693 - 27,916	n/a	2019	14	1
B27	MO 13 & MO 215, Brighton, MO	4-leg	15,300 - 20,839	1666-2211	2019	7	1
B28	MO 13 & 545th Road and MO 215, Brighton, MO	4-leg	15,300 - 20,839	1975-2661	2019	7	1
B29	MO 94 & South Breeze Lane, Weldon Spring, MO	4-leg	26,602 - 43,005	n/a	2019	14	1
B30	MO 13 & Route BB and Route CC, Alsup, MO	4-leg	15,300 - 23,593	1058-1154	2019	14	1
B31	MO 13 & Route WW, Springfield, MO	4-leg	18,579 - 24,242	1154-2724	2019	14	1
B32	MO 13 and State Highway O, Springfield, MO	4-leg	18,579 - 25,968	1524-2066	2019	14	1

*When minor-approach AADT data was not available, a default value of 200 vpd was used in the prediction model.

4.3.2 Results

The safety evaluation results of 32 J-turn intersections using the EB method are shown in Table 4-4. Among these, 22 J-turns demonstrated a reduction in FI crashes, as indicated by their CMS values being below 1.0 at 95% confidence level. Although two sites (B15 and B22) had CMF values greater than 1.0, neither was statistically significant. Overall, the CMF value of J-turns was 0.486, indicating a 51.4% reduction in FI crashes at J-turn intersections.

For FI (KAB), 23 sites demonstrated a significant reduction at the 95% confidence level. The CMF values for five sites were greater than 1.0, though none were statistically significant. The aggregated CMF value for all J-turn sites was 0.477, indicating a 52.3% reduction in FI (KAB) excluding possible injury crashes, close to the results observed for FI crashes.

For total crashes, 17 sites demonstrated a significant reduction at the 95% confidence level, but two sites (B1 and B15) experienced a significant increase. After reviewing the CMF calculations and crash data, the likely cause of the unexpectedly significant increase was identified as the lack of minor road AADT data. As noted in the previous data description, a default value of 200 vpd was used in the prediction model when minor-approach AADT data was unavailable, which could have resulted in inaccurate crash predictions. Despite these potential inaccuracies at a few sites, J-turns, overall, still exhibit a significant reduction in total crashes by 40.3% with a CMF value of 0.597.

The results from the empirical Bayes (EB) methods aligned with those from the Comparison Group (CG) method. For FI crashes, the CMFs were 0.534 (CG) and 0.486 (EB). For total crashes, the CMFs were 0.556 (CG) and 0.573 (EB). Two different safety methodologies, using related but different types of data, showed that the J-turn design could significantly reduce both FI and total crashes.

Table 4-4. Results of the empirical Bayes analysis.

#	FI observed after	Expected	CMF	St. E.	FI (KAB) observed after	Expected	CMF	St. E.	Total crash observed after	Expected	CMF	St. E.
B1	7	9.318	0.621	0.125	6	6.645	0.770*	0.209	59	31.204	1.747	0.154
B2	12	11.308	0.959*	0.189	11	8.577	1.161*	0.270	26	26.814	0.932*	0.126
B3	6	16.051	0.352	0.085	6	11.399	0.496	0.140	25	28.500	0.843*	0.112
B4	4	10.321	0.354	0.105	4	7.935	0.465	0.161	14	22.836	0.583	0.093
B5	12	25.506	0.445	0.068	11	17.810	0.584	0.111	34	54.861	0.604	0.058
B6	10	73.958	0.130	0.013	9	45.076	0.193	0.028	46	228.403	0.199	0.010
B7	10	9.107	0.660	0.143	8	12.377	0.611	0.153	33	18.215	1.751*	0.274
B8	18	30.468	0.573	0.087	17	25.162	0.655	0.111	93	185.420	0.497	0.026
B9	0	2.149	0.000	-	0	3.179	0.000	-	8	10.233	0.704*	0.160
B10	5	3.533	0.993*	0.314	5	2.466	1.453*	0.567	15	19.604	0.706	0.104
B11	8	6.812	0.955*	0.222	8	5.076	1.291*	0.358	28	49.019	0.536	0.040
B12	11	34.758	0.289	0.028	9	25.537	0.322	0.043	37	52.801	0.660	0.046
B13	9	7.769	0.942*	0.197	9	6.379	1.156*	0.276	23	25.113	0.855*	0.104
B14	10	11.946	0.813*	0.216	9	11.628	0.752*	0.209	42	58.627	0.709	0.081
B15	10	3.347	2.517*	0.830	10	3.238	2.615*	0.874	43	20.382	2.048	0.293
B16	8	15.42	0.502*	0.131	6	13.432	0.432	0.133	19	38.235	0.490	0.082
B17	1	9.94	0.096	0.066	1	7.225	0.132	0.100	6	34.521	0.169	0.038
B18	6	15.223	0.378	0.105	6	13.077	0.440	0.129	22	25.861	0.835*	0.143
B19	3	4.937	0.595*	0.320	1	5.644	0.174	0.159	25	32.089	0.773*	0.135
B20	2	2.923	0.640*	0.401	2	2.580	0.725*	0.464	13	11.082	1.153*	0.296
B21	1	7.347	0.134	0.122	1	7.045	0.140	0.128	9	15.327	0.583	0.180
B22	7	3.42	1.954*	0.734	5	2.222	2.151*	0.968	19	12.870	1.456*	0.318
B23	0	0.866	0.000	-	0	0.824	0.000	-	1	2.272	0.429*	0.411
B24	1	4.744	0.206	0.190	1	4.266	0.230	0.213	9	15.597	0.573	0.179
B25	0	3.863	0.000	-	0	3.069	0.000	-	0	8.292	0.000	-

#	FI observed after	Expected	CMF	St. E.	FI (KAB) observed after	Expected	CMF	St. E.	Total crash observed after	Expected	CMF	St. E.
B26	0	1.429	0.000	-	0	0.965	0.000	-	1	3.231	0.289	0.243
B27	0	1.655	0.000	-	0	1.408	0.000	-	4	3.744	1.032*	0.486
B28	1	2.513	0.378*	0.343	0	2.304	0.000	-	5	4.757	1.021*	0.429
B29	4	11.529	0.343	0.155	4	8.592	0.460	0.214	15	36.223	0.413	0.098
B30	0	1.954	0.000	-	0	1.465	0.000	-	5	6.473	0.760*	0.319
B31	0	1.888	0.000	-	0	1.760	0.000	-	0	4.287	0.000	-
B32	1	4.96	0.198	0.184	1	4.311	0.228	0.214	3	15.024	0.199	0.107
Total	167	353.680	0.486	0.027	150	314.235	0.477	0.028	682	1141.338	0.597	0.016

* Not significant at the 95% confidence level.

4.4 J-turn Crash Frequency Modeling

4.4.1 Data Description

Crash data of 32 J-turn intersections prepared for the EB safety evaluation, from 2005 to 2021, were also used to develop crash prediction models. However, exploratory data analysis revealed that intersections lacking minor road AADT data and using a default value of 200 vpd significantly increased variance in crash frequency modeling and were subsequently excluded. Furthermore, since all three three-leg J-turns lacked minor road AADT data, the crash frequency models were developed for four-leg J-turn intersections only. After excluding intersections without minor road AADT, the refined database of 144 annual records from 26 J-turn intersections (2005 to 2021) was used to develop the crash frequency models.

The crash frequency model used annual total crash frequency and annual FI crash frequency as dependent variables. The independent variables selected for the crash prediction modeling and their levels are detailed in Table 4-5.

Table 4-5. Definitions and levels of independent variables.

Independent Variable	Definition	Level
AADT	Major road AADT	3,788 – 33,755 vpd
Minor AADT	Minor road AADT	278 – 12,719 vpd
Loon	Presence of loon	0: not present 1: one loon 2: two loons
Left turn	Presence of left turn lane from mainline	0: not present/no left turn allowed 1: one left turn lane 2: two left turn lanes
Minor DL	Presence of deceleration lane (DL) for turning right to minor road	0: not present 1: one deceleration lane to minor road 2: two deceleration lanes to minor road
Minor AL	Presence of acceleration lane (AL) for turning right from minor road	0: not present 1: one acceleration lane from minor road 2: two acceleration lanes from minor road
Median DL	Presence of median deceleration lane before U-turn	0: not present 1: one median deceleration lane 2: two median deceleration lanes
Median AL	Presence of median acceleration lane after U-turn	0: not present 1: one median acceleration lane 2: two median acceleration lanes
Island	Presence of splitter island on minor approach	0: not present 1: one island on minor approach 2: two islands on minor approach

4.4.2 Results

4.4.2.1 Total Crash Frequency

The total crash frequency models were first developed, using the number of total crashes at J-turn intersections as the dependent variable. Independent variables were introduced to the crash model one at a time, and their functional forms were determined based on goodness-of-fit measures. The potential functional forms considered in the modeling process included offset, log-normalized, and exponent.

The first variable introduced into the crash frequency models was major road AADT, followed by minor road AADT, as traffic volumes have been considered as significantly impacting crash prediction models for intersections (AASHTO 2010). The functional forms for both variables were compared, and the optimal form was presented in Equation 4.1, which was consistent with the intersection equation of the HSM (AASHTO 2010). The equation serves as the foundation for other variables.

$$N_{total} = \exp\left[\left(\alpha + \beta_1 \times \ln(AADT) + \beta_2 \times \ln(Minor\ AADT)\right]\right.$$

The parameters and goodness-of-fit measures are shown in Table 4-6. The results showed that including the variable of Minor AADT improved all the four measures, as the R^2_{adj} value increased from 0.497 to 0.549, while the k, MAD, and AIC values decreased. The MAD measure indicated that the average annual error in crash prediction per intersection is +/- 1.638 crashes/year.

Table 4-6. Total crash frequency models using AADT and minor AADT.

#	Variable	Functional form	α	p-value	β_1	p-value	β_2	p-value	K	R^2_{adj}	MAD	AIC
1	ln(AADT)	Exponent	-8.727	0.011	1.037	0.143	-	-	0.168	0.497	1.694	539.003
2	ln(AADT), ln(Minor AADT)	Exponent	-10.422	0.012	1.021	0.142	0.243	0.082	0.144	0.549	1.638	532.560

Figure 4-1 shows the CURE plots for the variables of AADT and Minor AADT. The results showed that the cumulative residuals fell into the +/- 2σ boundary and indicated a consistent fit of the data across the model function forms.

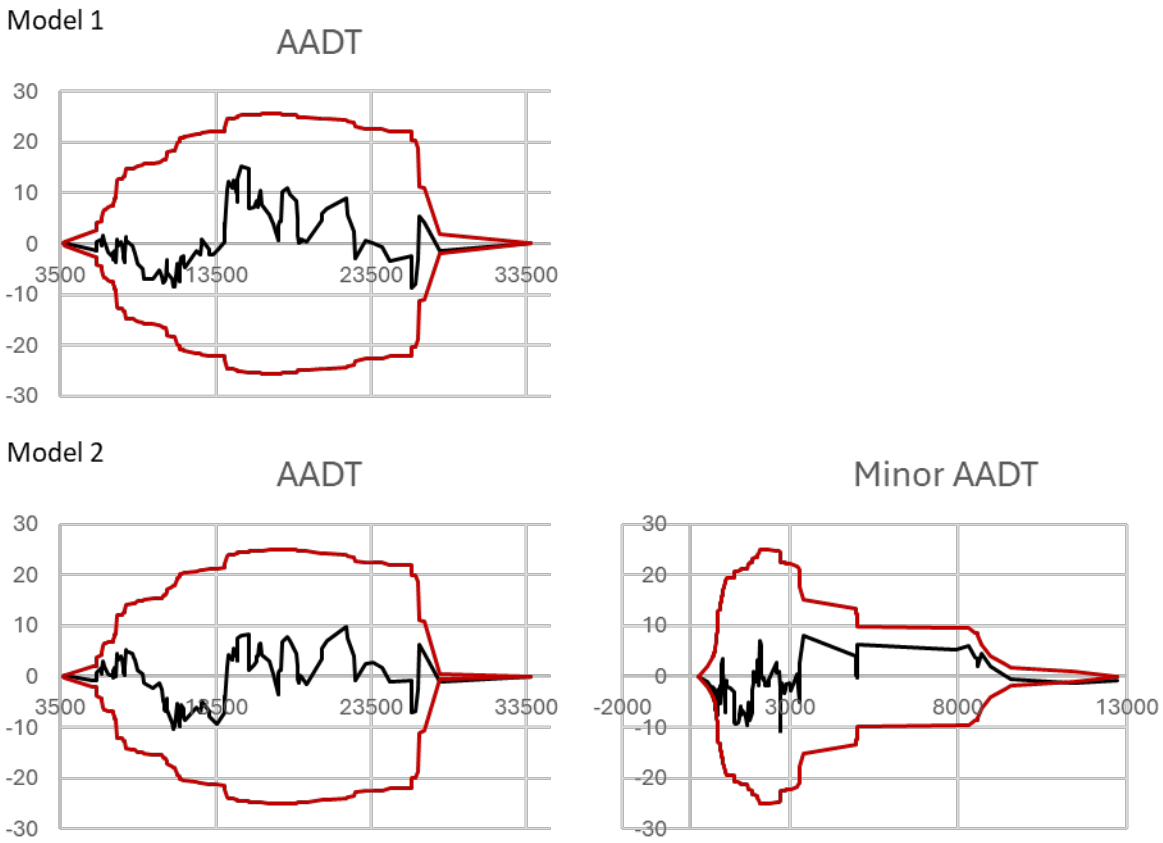

Figure 4.1. CURE plots of total crash frequency models for AADT and minor AADT.

After developing the foundational model using major road and minor road AADTs, the crash frequency models were developed by introducing an additional intersection-related variable. The results of the development, including functional form of the newly added variable, parameters, p-value of parameters, k, R^2_{adj}, MAD, AIC, and the CMF value of the newly added variable are detailed in Table 4-7. The results showed that the introduction of new variables generally enhanced the accuracy of the foundational model. Among the developed eight new models, the model with the variable of Minor AL improved all four measures and was considered the optimal model with three variables.

The CURE plots of AADT and minor AADT for each total crash model are shown in Figure 4-2. Overall, the CURE plots showed that all eight models newly developed with an additional variable indicated a good fit for the data.

The value of β_3 indicates the impact of newly added factors on the total number of crashes. A value smaller than zero suggests that the total number of crashes will decrease with an increase in the value of the variable. A β_3 value greater than zero indicates an increase in crashes due to an increase in the value of the variable. The results showed that most J-turn design elements

had a β_3 value smaller than zero indicating a reduction in crashes to varying degrees. The magnitude of β_3 reflects the degree of impact of the variables on crashes. The β_3 value for left turn lanes on the mainline was greater than zero. This was expected as the left turn lanes were mainly provided at sites with high left turning volumes.

Table 4-7. Total crash frequency modeling development.

#	New Variable	Form of added variable	β_1	p-value	β_2	p-value	β_3	p-value	K	R^2_{adj}	MAD	AIC
1	Loon	Exponent	0.952	0.175	0.269	0.091	-0.056	0.087	0.141*	0.562*	1.633*	534.161
2	Left turn	Exponent	1.061	0.145	0.229	0.082	0.235	0.197	0.136*	0.576*	1.641	533.199
3	Minor DL	Exponent	0.993	0.143	0.285	0.088	-0.201	0.166	0.137*	0.570*	1.625*	533.102
4	Minor AL	Exponent	1.135	0.157	0.297	0.087	-0.130	0.078	0.133*	0.582*	1.629*	531.789*
5	Median DL	Exponent	0.999	0.144	0.267	0.086	-0.105	0.122	0.140*	0.559*	1.638*	533.828
6	Median AL	Exponent	1.046	0.145	0.249	0.080	-0.097	0.090	0.136*	0.578*	1.631*	533.375
7	Island	Exponent	1.018	0.141	0.274	0.088	-0.192	0.223	0.140*	0.559*	1.635*	533.828

* Indicate that the newly added variable enhanced the existing model.

(1) Loon

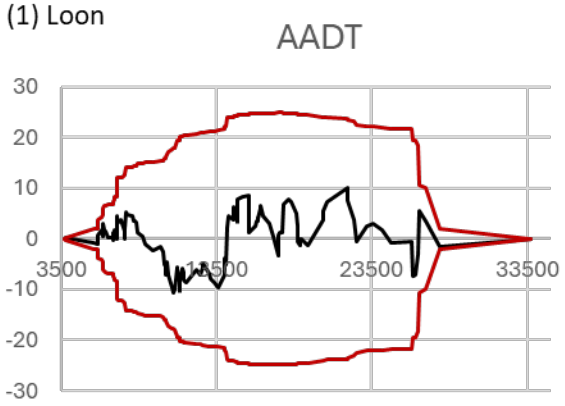

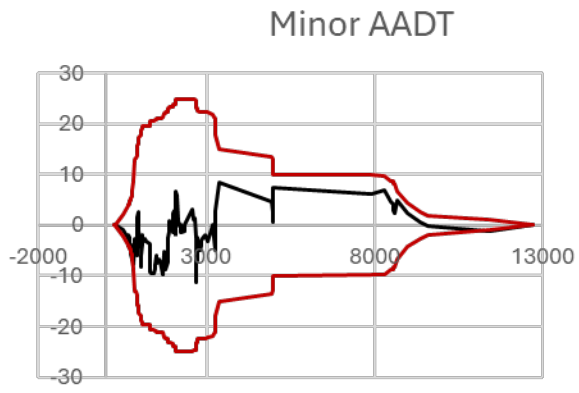

(2) Left turn

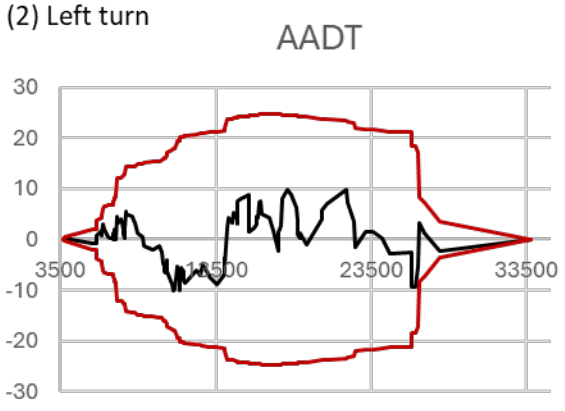

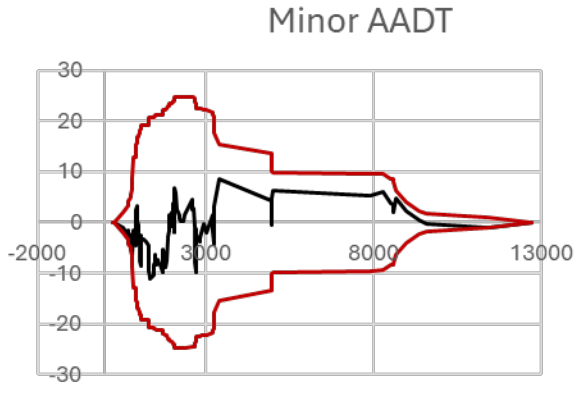

(3) Minor DL

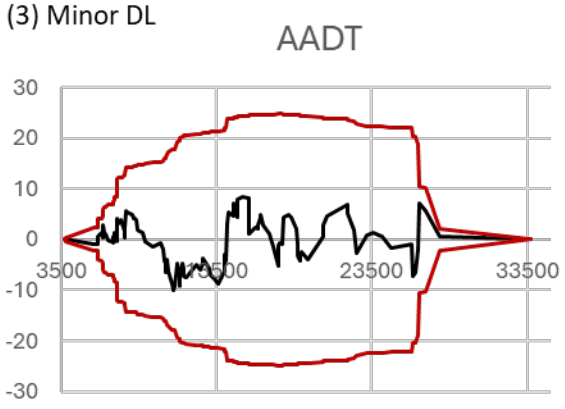

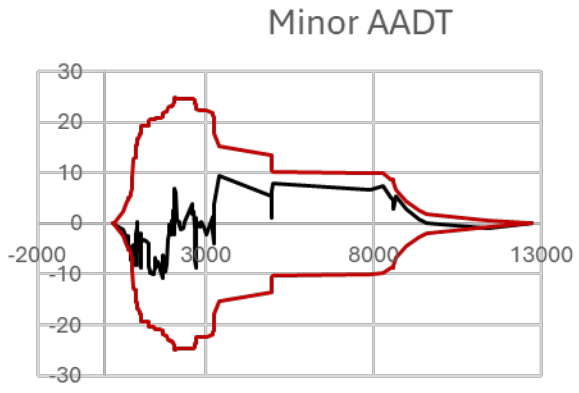

(4) Minor AL

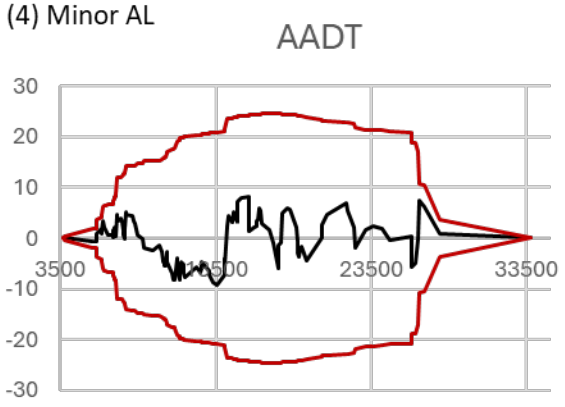

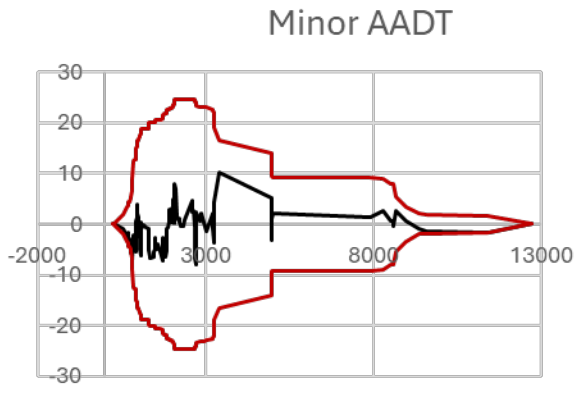

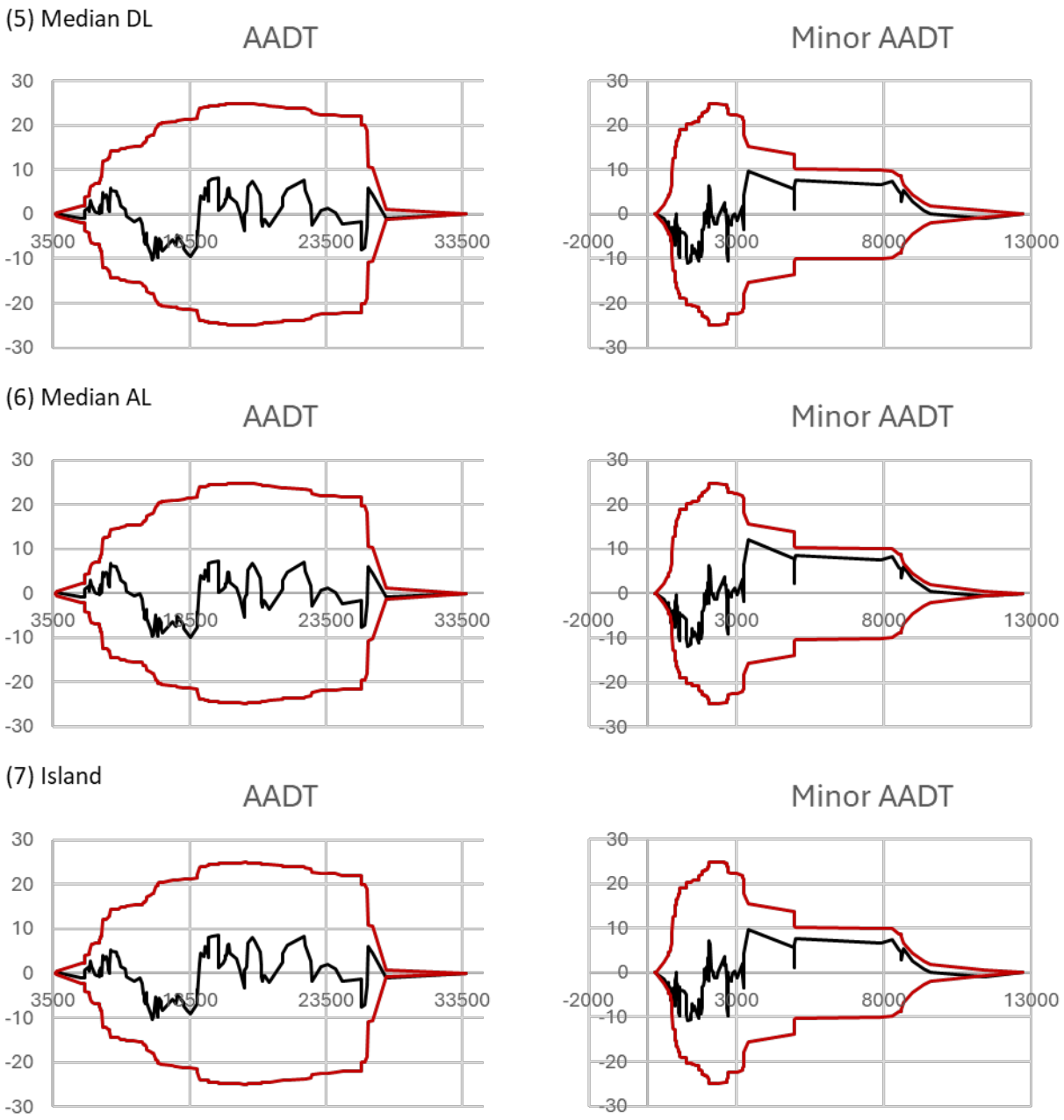

Figure 4.2. CURE Plots of total crash frequency models with new variables for AADT and minor AADT.

4.4.2.2 Fatal and Injury Crash Prediction

The FI crash frequency models were also developed, using the annual number of FI crashes at J-turn as the dependent variable. The first variable introduced into the crash frequency models was major road AADT, followed by minor road AADT. The developed models for AADT and Minor AADT used an exponent model in Equation 4.2, which was also consistent with the intersection equation used in the HSM (ASSHTO 2010).

$$N_{FI} = \exp\left[\ (\alpha + \beta_1 \times \ln(AADT) + \beta_2 \times \ln(Minor\ AADT)\right]$$

The parameters and goodness-of-fit measures of the models are shown in Table 4-8. The results showed that including the variable of Min AADT improved all four measures. The R^2_{adj} increased from 0.254 to 0.282, while the k, MAD, and AIC values decreased. The MAD measure indicated that the average annual error in crash prediction per intersection is +/- 0.831 crashes/year. The overall accuracy of FI crash frequency models was lower compared to the total crash models, due to the limited number of FI crashes observed (131 recorded) in the refined dataset.

Table 4-8. Fatal and injury crash frequency models using AADT and minor AADT.

#	Variable	Functional form	α	p-value	β_1	p-value	β_2	p-value	K	R^2_{adj}	MAD	AIC
1	ln(AADT)	Exponent	-8.328	0.239	0.859	0.251	-	-	0.371	0.254	0.837	326.458
2	ln(AADT), ln(Minor AADT)	Exponent	-9.976	0.263	0.845	0.253	0.234	0.146	0.348	0.282	0.831	325.939

The CURE plots for the foundational models with traffic volumes are shown in Figure 4.3. The results showed that approximately 4% of the cumulative residual exceeded the limits when AADT was around 6500 vpd and the minor AADT was around 700 vpd. The CURE plots also suggested that there was a sparse sample size for instances where the minor AADT exceeded than 3000 vpd. Overall, most of the cumulative residuals were still within the 95% confidence interval and there were no long trends, suggesting a reasonably good fit of the data.

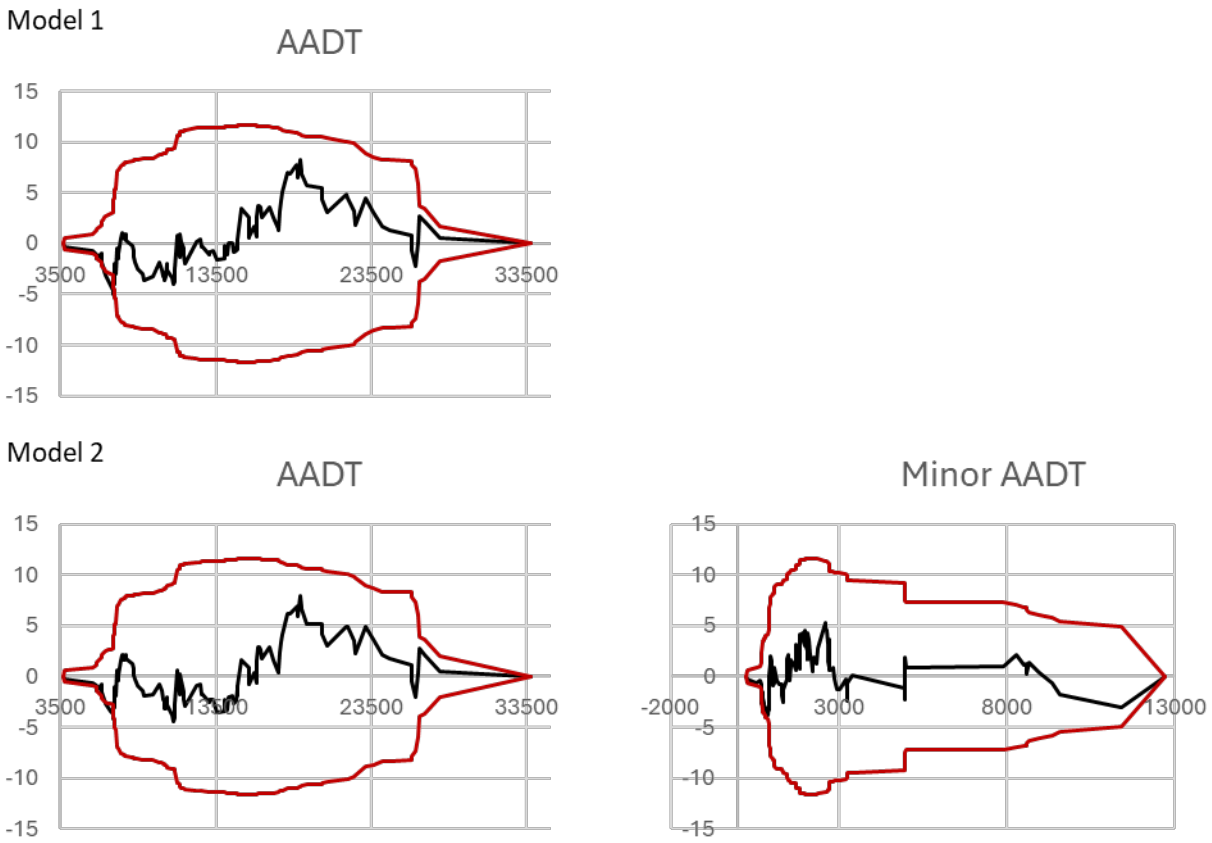

Figure 4.3. FI crash CURE plots for AADT and minor AADT.

After developing the foundational model using major road and minor road AADTs, the crash frequency models were also developed by introducing an additional intersection-related variable. The results of the development are detailed in Table 4-9. The results showed that the introduction of new variables generally enhanced the accuracy of the foundational model, especially with the variables of loon, minor DL, minor AL, and median DL, as all four measures with these variables improved. However, there was an exception for left turn lanes, which did not enhance the model in any measures.

The CURE plots of AADT and minor AADT for each total crash model are shown in Figure 4.4. The CURE plots showed that the models with intersection related variables were similar to the foundational model, where the prediction values exceeded the 95% confidence interval when the AADT is near 6500 vpd and the minor AADT is around 700 vpd. Except those sections, the CURE plots indicate a relatively good fit of the data.

The parameters from the regression model for FI crashes are shown in Table 4-9. Unlike the parameters for total crashes shown in Table 4-7, the smaller number of observed crashes (131 FI vs 412 total) meant that the p-values for the estimated parameters were higher as shown in

Table 4-9. Thus, we do not recommend using the β_3 parameters for the FI model shown in Table 4-9 due to their poor statistical significance.

Table 4-9. Fatal and injury crash frequency modeling development.

#	New Variable	Form of added variable	B_1	p-value	B_2	p-value	B_3	p-value	K	R^2_{adj}	MAD	AIC
1	Loon	Exponent	0.415	0.327	0.395	0.162	-0.329	0.161	0.281*	0.407*	0.812*	323.876*
2	Left turn	Exponent	0.820	0.263	0.244	0.148	-0.138	0.321	0.352	0.260	0.831	327.779
3	Minor DL	Exponent	0.764	0.255	0.355	0.156	-0.521	0.286	0.298*	0.355*	0.811*	324.794*
4	Minor AL	Exponent	1.082	0.276	0.347	0.157	-0.275	0.140	0.306*	0.314*	0.828*	324.285*
5	Median DL	Exponent	0.772	0.258	0.307	0.153	-0.295	0.202	0.311*	0.363*	0.820*	325.923*
6	Median AL	Exponent	0.863	0.258	0.238	0.144	-0.086	0.163	0.335*	0.315*	0.827*	327.656
7	Island	Exponent	0.836	0.251	0.303	0.158	-0.414	0.384	0.322*	0.340*	0.824*	326.803

* Indicate that the newly added variable enhanced the existing model.

(1) Loon

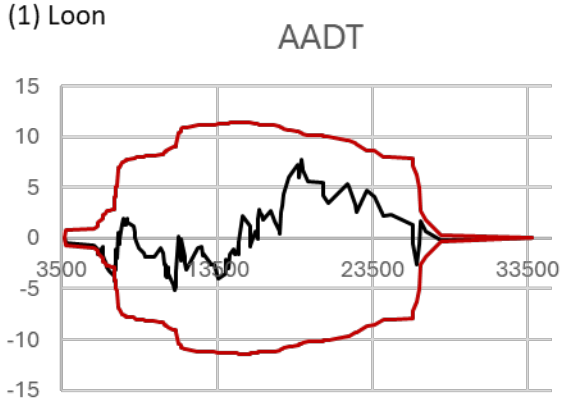

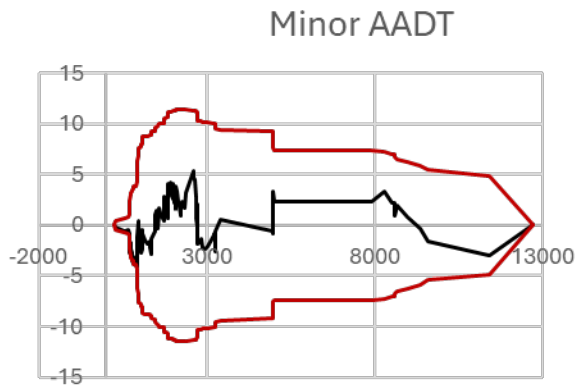

(2) Left turn

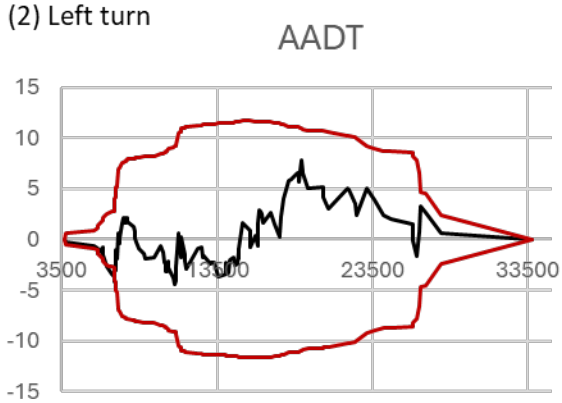

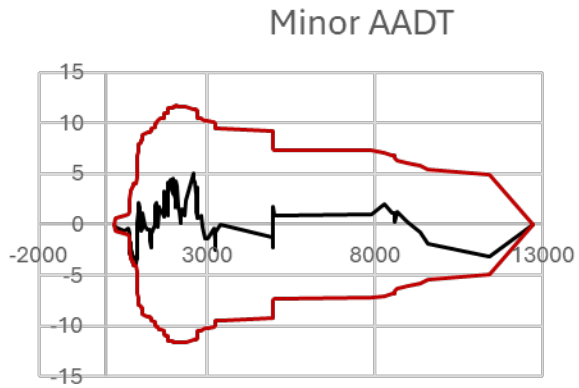

(3) Minor DL

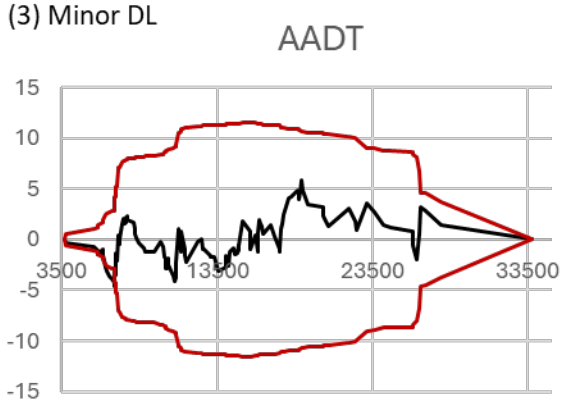

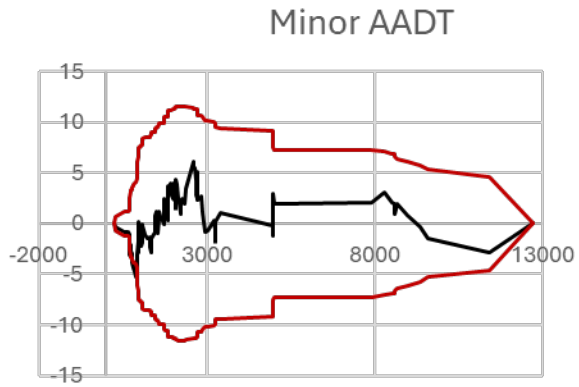

(4) Minor AL

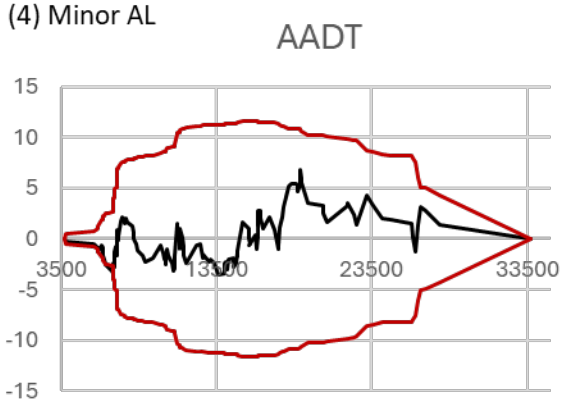

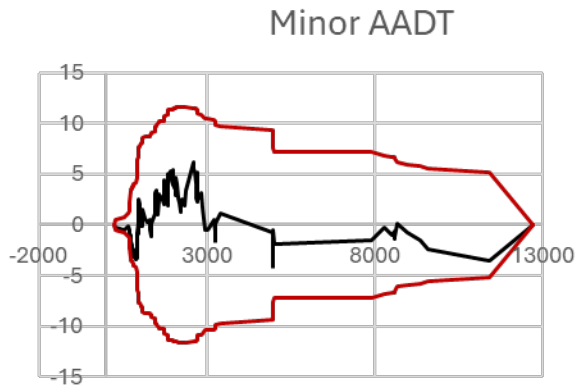

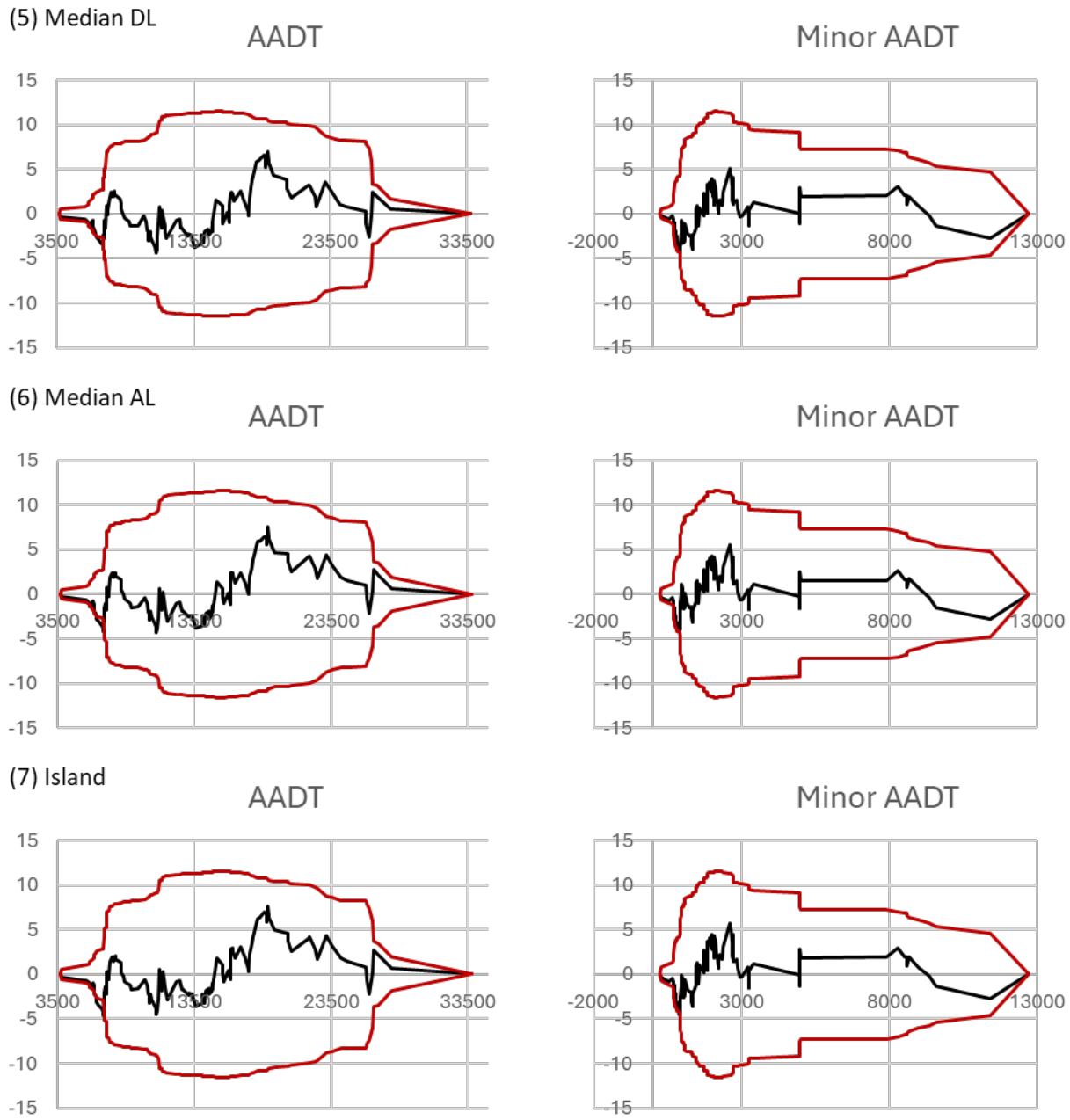

Figure 4.4 CURE Plots for FI crash frequency models with new variables.

4.5 Collision Diagram Analysis

The crash reports from 47 J-turn intersections from 2005 to 2021 were thoroughly reviewed and used to generate collision diagrams. These reports included crashes occurring within a 250-foot radius extending from the J-turn to minor roads, and also 250 feet beyond the U-turn locations. The distribution of crash types before and after the installation of J-turns is detailed in Table 4-

10. The differing numbers of total crashes before and after installation were influenced by the impact of J-turn installations and the availability of crash data, given the varying installation times. The three most common crash types after J-turn installation were out-of-control (35.9%), rear-end (21.5%), and sideswipes (13.2%). Before the J-turn installation, the predominant three types were right-angle (27.5%), rear-end (23.9%), and out-of-control (20.7%).

The crash data supports findings from previous research (Hallmark et al. 2016; Claros et al. 2017), showing a significant reduction in right-angle crashes from 27.5% to 8.2%, and a reduction in left turn crashes from 8.8% to 4.2%. These changes are due to the restricted left turn and through movements on minor roads. Concurrently, there has been an increase in sideswipes collision. The shifts in the distribution of crash types suggest that J-turns not only reduce the total number of crashes at intersections but also mitigate the severity of injuries. This is evidenced by the fact that 59% of FDI crashes were right-angle and left-turn collisions.

Table 4-10. Crash count and percentage by crash type before and after J-turn installation.

#	Type of crash	Crash count before J-turn installation	Percentage of the total before installation	Crash count after J-turn installation	Percentage of the total after installation	Trend
1	Out-of-control	577	20.7%	259	35.9%	↑
2	Rear-end	666	23.9%	155	21.5%	↓
3	Sideswipes*	66	2.4%	95	13.2%	↑
4	Animal collisions	216	7.8%	83	11.5%	↑
5	Right-angle	765	27.5%	59	8.2%	↓
6	Left turns	244	8.8%	30	4.2%	↓
7	Passing	170	6.1%	19	2.6%	↓
8	Right turns	50	1.8%	16	2.2%	→
9	Head-on	27	1.0%	5	0.7%	→
	Total	2781	100%	721	100%	

* The crash type of sideswipe includes both same-direction and opposite-direction sideswipe crashes.

The collision location diagrams were examined for each type of crash. Out-of-control crashes, being the most common type, are shown in Figure 4.5. While out-of-control crashes can occur randomly within J-turns due to various factors, such as road debris, weather conditions, and driver negligence, they most frequently occurred near the margining areas between highways and minor roads. Specifically, 124 out of the 259 total out-of-control crashes occurred in these merging areas. Nearly 85% of out-of-control crashes in the area were caused by failure to reduce speed, often due to driver negligence or weather conditions, while the remaining 15% were related to slow traffic.

Figure 4.6 illustrates the locations of rear-end crashes, which are the second most frequent type of crash. Rear-end collisions often occur due to significant speed differentials between vehicles or the sudden stop of the leading vehicle; Over 40% of these crashes took place near the points where traffic from minor roads stopped and merged onto the mainline. Additionally, approximately 30% rear-end crashes occurred near the entrances to deceleration lanes or at the end of acceleration lanes.

Sideswipe crashes can be further divided into same-direction and opposite-direction sideswipe. Figure 4.7 shows that same-direction sideswipe crashes primarily occurred along the highway stretch from the deceleration lane entrance for minor roads to the median acceleration lane before the U-turns. Notably, only seven of these crashes took place near the U-turns. Figure 4.8 shows that the locations of opposite-direction sideswipe crashes, primarily occurring on minor roads before traffic merges onto the highway. Only two such collisions took place on highways, where one of the vehicles crossed the center line and entered the opposing traffic.

Located primarily in rural areas, animal collisions emerged as the fourth most common type of crash at J-turns. These collisions may not be directly related to the J-turns intersection-related characteristics, as they occurred randomly across the J-turn intersection (Figure 4.9).

Figure 4.10 illustrates that most right-angle crashes occurred at the intersection where highway traffic turns left to enter minor roads, with 49 out of 59 crashes concentrated in this area. In contrast, only five right-angle crashes occurred near the U-turns.

Figure 4.11 shows the locations of these left turn crashes. There were 30 recorded left turn crashes, with 22 of these occurring where vehicles turn left from the highway to enter minor roads. Additionally, four left turn crashes happened near the U-turns. As the common cause for both right-angle and left-turn crashes is that left-turn driver failed to yield the right of way or misjudged the gap, the two types of crashes often occur in the same areas.

Figure 4.12 illustrates the locations of passing-related crashes. Of the 19 incidents recorded, 11 occurred near the beginning or end of acceleration and deceleration lanes, where lanes merge or diverge. This complexity in driving maneuvers heightens the risk of collisions during passing.

Figure 4.13 documents the locations of right-turn crashes. Of the 16 reported incidents, 14 occurred as vehicles made right turns to enter the highway from minor roads, while two crashes happened when vehicles attempted to turn right into minor roads.

Figure 4.14 illustrates the locations of five head-on crashes. Two crashes occurred on minor roads. One crash was atypical, caused by a vehicle losing control and rotating, resulting in a head-on collision. Another crash involved a vehicle from the minor road attempting to make a U-turn back to the minor road at the intersection. The final crash was a wrong-way head-on collision, but it was not able to determine when the driver began traveling in the wrong direction.

Lastly, Figure 4.15 highlights the most frequent crash locations and their percentage of total crashes for each type of crash. The figure helps identify the hot spots and scenarios typically associated with these crashes. The diagram indicates that the majority of crashes still occurred in areas where minor road traffic merges onto highways, rather than at U-turn locations.

The observed crash locations also suggest how J-turn characteristics can mitigate risks. For example, according to results from J-turn crash frequency models, one effective strategy to decrease rear-end collisions is to install acceleration lanes for turning right traffic from minor roads, which help align the speeds of merging traffic with that of the mainline flow.

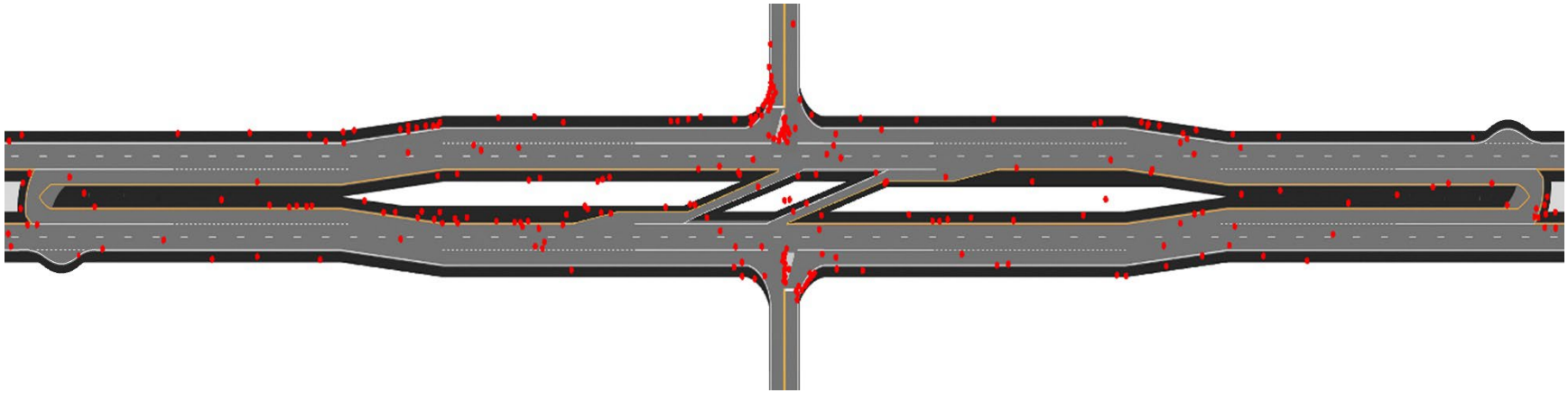

Figure 4.5. Out-of-control collision location analysis.

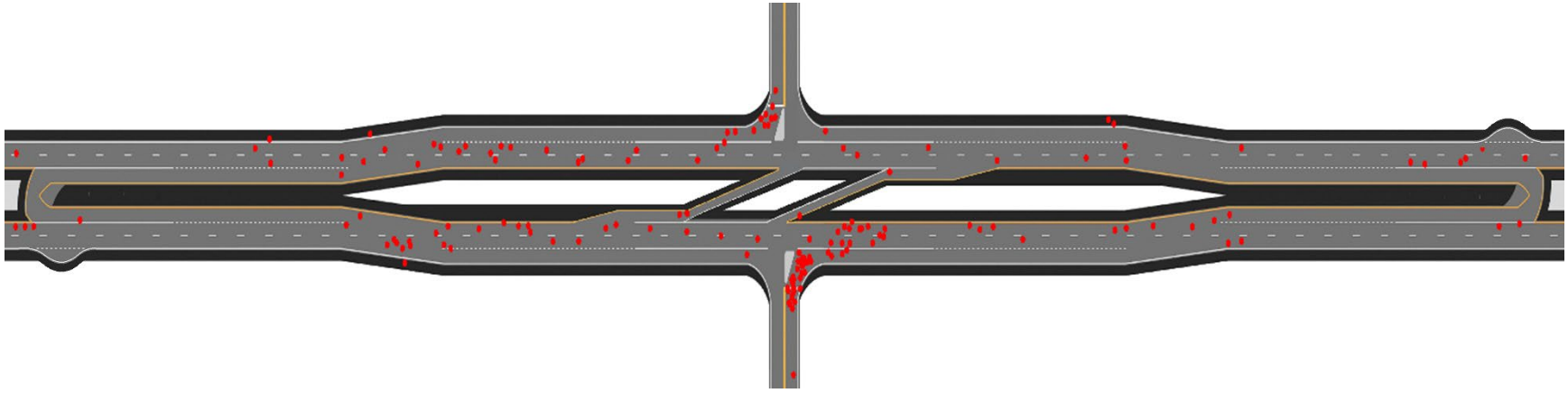

Figure 4.6. Rear-end collision location analysis.

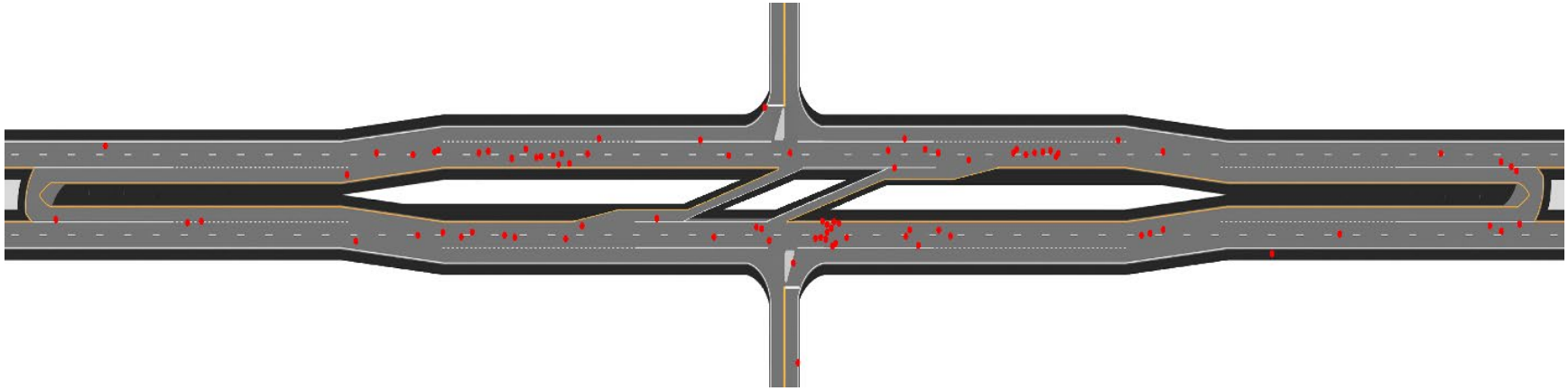

Figure 4.7. Same-direction sideswipe collision location analysis.

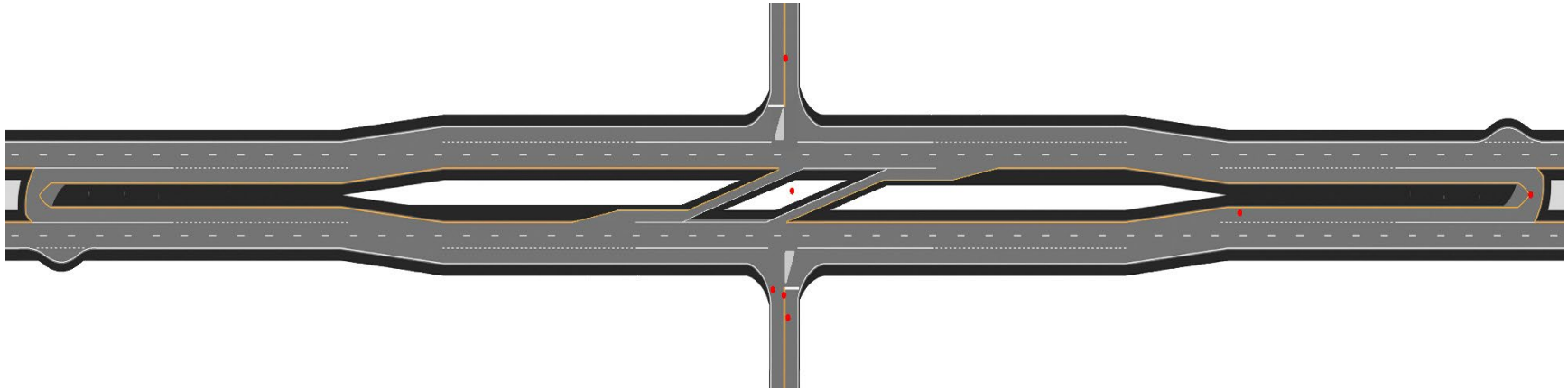

Figure 4.8. Opposite-direction sideswipe collision location analysis.

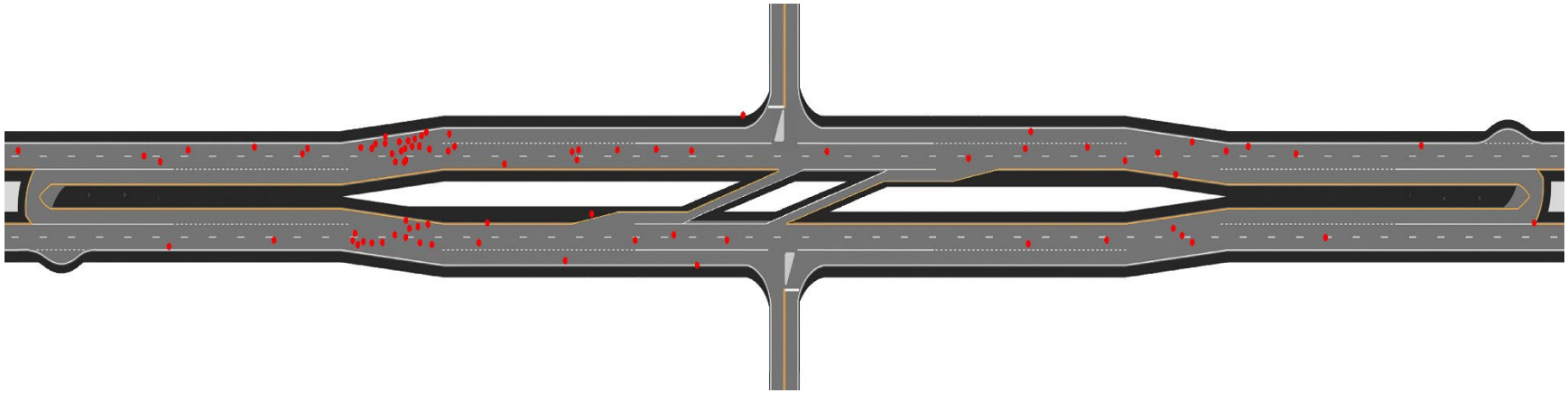

Figure 4.9. Animal collision location analysis.

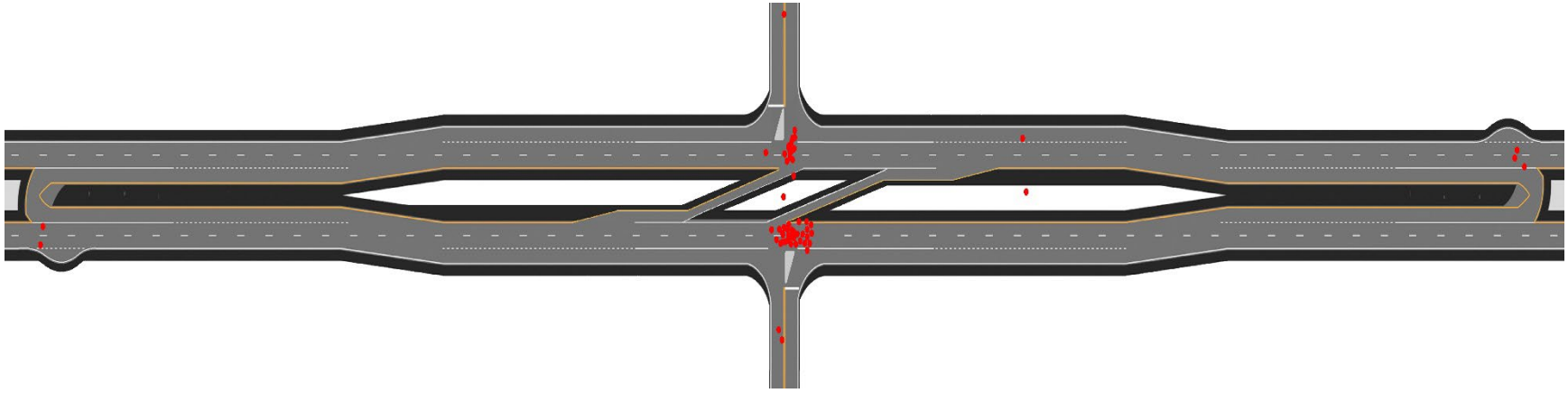

Figure 4.10. Right angle collision location analysis.

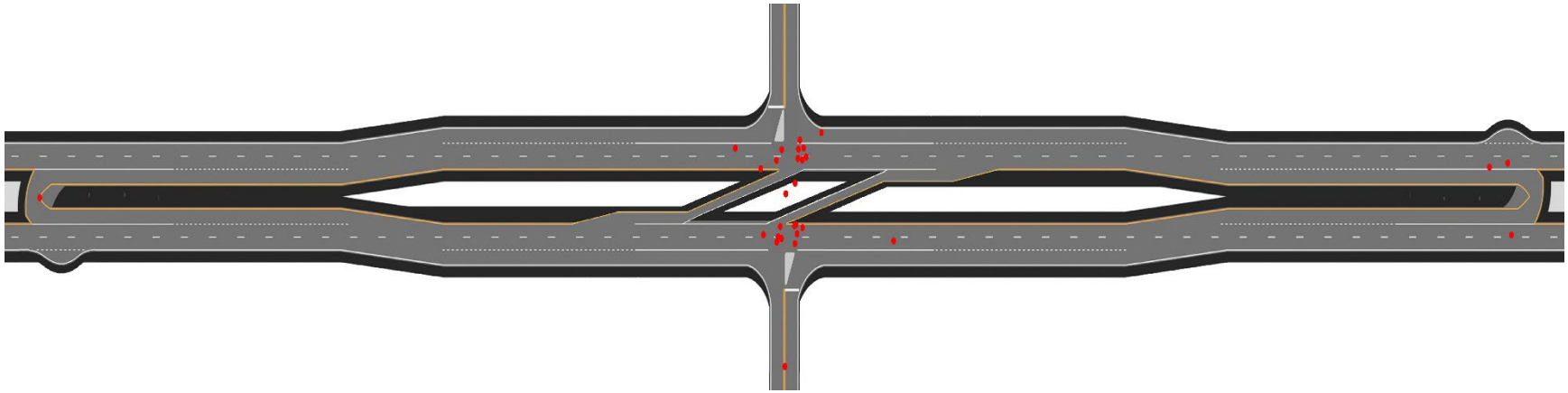

Figure 4.11. Left turn collision location analysis.

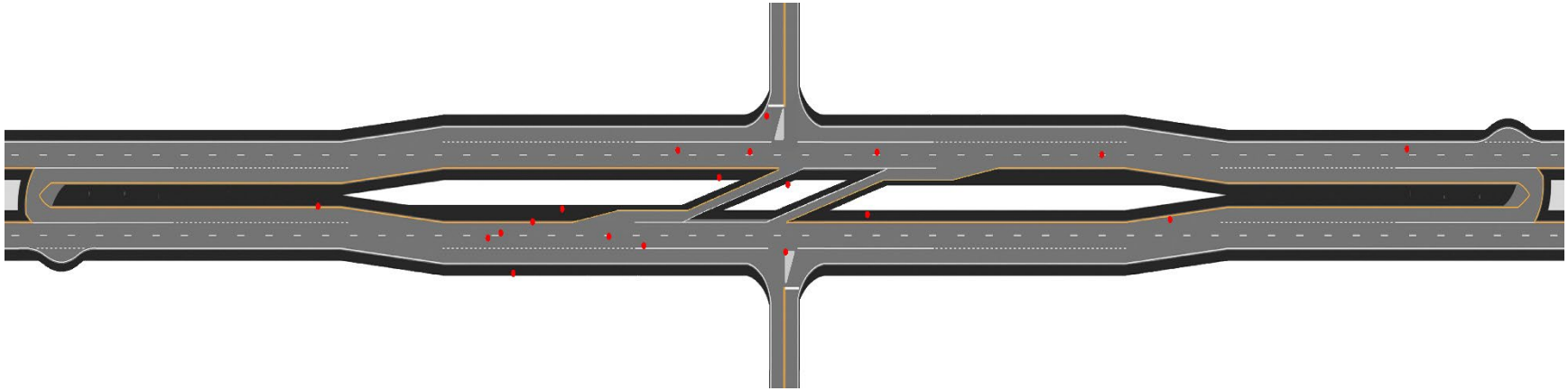

Figure 4.12. Passing collision location analysis.

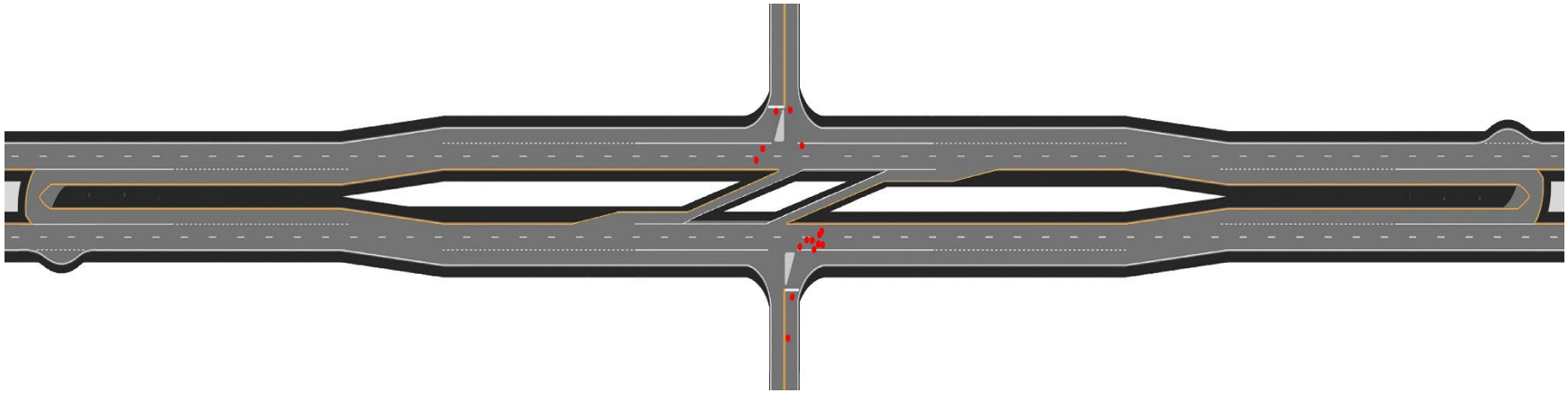

Figure 4.13. Right turn collision location analysis.

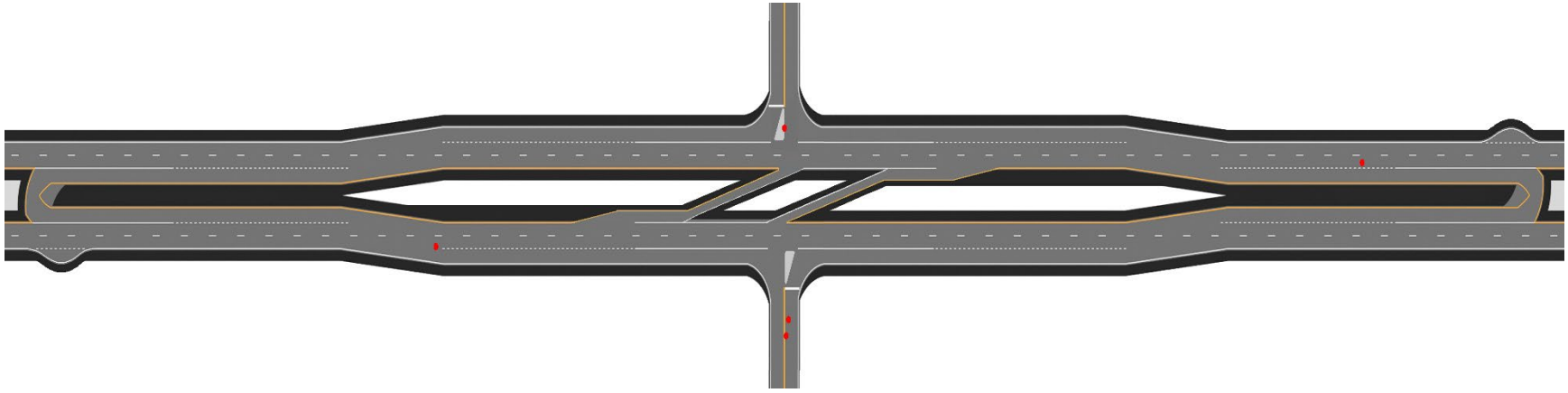

Figure 4.14. Head-on collision location analysis.

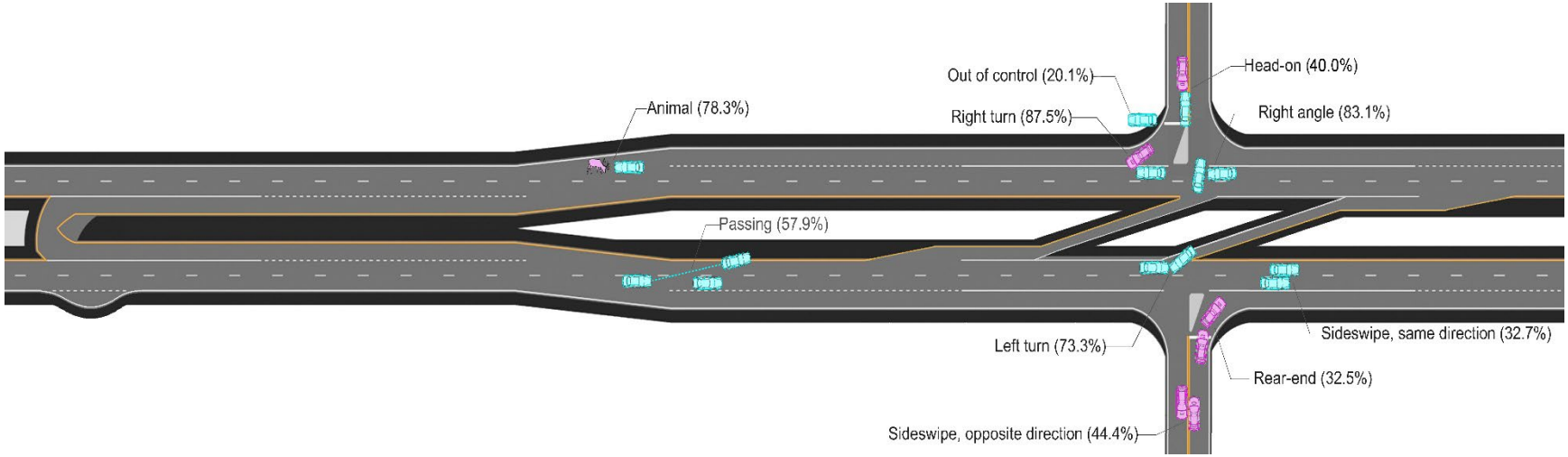

Note: The number in parentheses indicates the percentage of the same type of crashes that occurred in similar locations.

Figure 4.15. Most frequent crash location for each type of crash.

5. CONCLUSIONS

This study evaluated the safety performance of J-turn intersections in Missouri using 47 J-turns and 20 comparison intersections. The safety effectiveness of J-turns was evaluated through two different methods, the CG and EB before-after method. Further, the safety impact of J-turn-related characteristics, such as acceleration/deceleration lanes and islands, were explored through crash frequency modeling. Lastly, collision diagrams were generated to gain additional insight into crash types and locations. The following are the key findings of this study.

- The CG analysis, which examined 20 paired J-turns and stop-controlled intersections, demonstrated that J-turns reduced total crashes by 44.4%, FI crashes by 46.6% and FDI crashes by 74.5%.
- The EB before-after analysis also confirmed the safety benefits of J-turns, showing reductions of 51.4% in FI crashes, 52.3% in FI (KAB) crashes, and 40.3% in total crashes.
- The crash frequency models developed using crash data only from J-turn sites indicated the positive impact of different design elements such as loons, deceleration/acceleration lanes, and separate islands. Since left turn lanes were typically provided at high traffic locations, the model showed that J-turn sites with left turn lanes on the mainline experienced higher crashes than at sites with lower traffic and no left turn lanes.
- The collision diagram analysis showed a shift from right-angle and left-turn collisions at traditional two-way stop-controlled intersections to sideswipe collisions at J-turns. Most crashes occurred where minor road traffic merged onto the major road. The observed crash locations also suggest how J-turn designs, such as acceleration/deceleration lanes can effectively mitigate risks.

In conclusion, the results from this study provide robust evidence of safety benefits of converting traditional intersections to J-turns on rural high-speed highways. The study generated CMFs and collision diagrams that can be used by MoDOT engineers as they consider J-turn design as a safety countermeasure.

REFERENCES

AASHTO. 2010. *Highway Safety Manual*. Washington, D.C. AASHTO.

Al-Omari, Ma'en Mohammad Ali, Mohamed Abdel-Aty, Jaeyoung Lee, Lishengsa Yue, and Ahmed Abdelrahman. 2020. "Safety Evaluation of Median U-Turn Crossover-Based Intersections." *Transportation Research Record* 2674 (7): 206–18.

Claros, Boris, Zhongyuan Zhu, Praveen Edara, and Carlos Sun. 2017. "Design Guidance for J-Turns on Rural High-Speed Expressways." *Transportation Research Record* 2618 (1): 69–77.

Edara, Praveen, Sawyer Breslow, Carlos Sun, and Boris R Claros. 2015. "Empirical Evaluation of J-Turn Intersection Performance: Analysis of Conflict Measures and Crashes." *Transportation Research Record* 2486 (1): 11–18.

Gross, Frank, Bhagwant Naraine Persaud, and Craig Lyon. 2010. "A Guide to Developing Quality Crash Modification Factors." United States. Federal Highway Administration. Office of Safety.

Hallmark, Shauna, Neal Hawkins, Raju Thapa, Skylar, and Knickerbocker. 2016. "MnDOT Evaluation of Truck and Agricultural Vehicle Behavior at Reduced Conflict Intersections." Institute for Transportation Iowa State University. https://intrans.iastate.edu/research/completed/mndot-evaluation-of-truck-and-agricultural-vehicle-behavior-at-reduced-conflict-intersections/.

Hauer, Ezra. 1997. *Observational Before/After Studies in Road Safety. Estimating the Effect of Highway and Traffic Engineering Measures on Road Safety*.

Hauer, Ezra. 2015. *The Art of Regression Modeling in Road Safety*. Vol. 38. Springer.

Hochstein, Joshua Lee, Thomas H. Maze, Tom Michael Welch, Howard Preston, and Richard Storm. 2009. "J-Turn Intersection: Design Guidance and Safety Experience." https://trid.trb.org/View/880685.

Hummer, Joseph E, Rebecca L Haley, Sarah E Ott, Robert S Foyle, and Christopher M Cunningham. 2010. "Superstreet Benefits and Capacities."

Hummer, Joseph E, and Sathish Rao. 2017. "Safety Evaluation of Signalized Restricted Crossing U-Turn Intersections." United States. Federal Highway Administration. Office of Safety Research and Development.

Inman, Vaughan W, and Robert P Haas. 2012. "Field Evaluation of a Restricted Crossing U-Turn Intersection." United States. Federal Highway Administration. Office of Safety Research and Development.

Leuer, Derek, and Katie Fleming. 2017. "A Study of the Traffic Safety at Reduced Conflict Intersections in Minnesota."

Lu, Jian, S Dissanayake, and L Xu. 2001. "Safety Evaluation of Right Turns Followed by U-Turns as an Alternative to Direct Left Turns: Crash Data Analysis."

Maze, Tom H, Joshua L Hochstein, Reginald R Souleyrette, Howard Preston, and Richard Storm. 2010. *Median Intersection Design for Rural High-Speed Divided Highways*.

Mishra, Raunak, and Srinivas S Pulugurtha. 2022. "Safety Evaluation of Unsignalized and Signalized Restricted Crossing U-Turn (RCUT) Intersections in Rural and Suburban Areas Based on Prior Control Type." *IATSS Research* 46 (2): 247–57.

Srinivasan, Raghavan, and Karin M Bauer. 2013. “Safety Performance Function Development Guide: Developing Jurisdiction-Specific SPFs.” United States. Federal Highway Administration. Office of Safety.

Sun, Carlos, Praveen Edara, Henry Brown, Jacob Berry, Boris Claros, and Xiang Yu. 2018. “Missouri Highway Safety Manual Recalibration.”

Sun, Xiaoduan, and M Ashifur Rahman. 2019. “Investigating Safety Impact of Center Line Rumble Strips, Lane Conversion, Roundabout, and J-Turn Features on Louisiana Highways.” Louisiana Transportation Research Center.

Ulak, Mehmet Baran, Eren Erman Ozguven, Hasan Huseyin Karabag, Mahyar Ghorbanzadeh, Ren Moses, and Maxim Dulebenets. 2020. “Development of Safety Performance Functions for Restricted Crossing U-Turn Intersections.” *Journal of Transportation Engineering, Part A: Systems* 146 (6): 04020038.

APPENDIX: J-turn Intersections in Missouri

Table A-1. J-turn locations and installation date.

#	Major Road	Minor Road	Installation
1	US 63	Old Millers Road, Columbia, MO	9/26/2012
2 [EB]	RT M	Old Lemay Ferry Connector, Barnhart, MO	8/27/2007
3 [CG EB M]	US 54	Route E, Jefferson City, MO	8/9/2012
4 [CG EB M]	US 54	Honey Creek Road, Jefferson City, MO	8/9/2012
5 [EB]	US 54	Route CC, Jefferson City, MO	8/9/2012
6 [EB M]	US 54	Buffalo Road, Heritage Highway, Jefferson City, MO	8/9/2012
7 [CG EB M]	MO 30	Osage Executive Drive, Byrnes Mill, MO	10/13/2012
8 [CG EB M]	US 65	Rochester Road, Ridgedale, MO	11/15/2012
9 [CG EB]	US 63	Route AB, Columbia, MO	9/26/2012
10 [CG EB M]	US 65	Red Top Road and Route EE, Buffalo, MO	12/1/2009
11 [CG EB M]	US 65	MO 215, Fair Grove, MO	12/1/2009
12 [CG EB M]	US 65	Red Top Road and Route AA, Fair Grove, MO	12/1/2009
13 [CG EB M]	MO 13	Northeast Old Highway 13, Osceola, MO	11/15/2008
14 [CG EB M]	US 65	MO 38, Buffalo, MO	12/1/2009
15 [CG EB]	US 63	Hinton Road and Calvert Hill Road, Columbia, MO	11/11/2014
16 [CG EB]	US 63	Peterson Lane, Ashland, MO	10/30/2014
17 [CG EB M]	US 50	MO 58, Centerview, MO	9/9/2014
18 [CG EB M]	US 63	Main Street and Route M, Atlanta, MO	11/13/2014
19 [CG EB M]	US 63	Route P, Route B, Clark, MO	11/14/2014
20 [CG EB M]	US 50	MO 131, Holden, MO	8/15/2017
21 [CG EB M]	US 67	New Perrine Road, Farmington, MO	11/6/2018
22 [EB M]	MO 13	Route Y and Route U, Bolivar, MO	12/5/2018
23 [CG EB]	US 50	S Buckner Tarsney Road, Lone Jack, MO	10/26/2018
24 [EB M]	MO 13	Calvird Drive, Clinton, MO	11/15/2019
25 [CG EB M]	US 54	Route A, Linn Creek, MO	6/3/2019
26 [EB M]	MO 13	MO 123, Humansville, MO	11/15/2019
27 [CG EB M]	US 54	Old US 54, Osage Beach, MO	6/3/2019
28 [EB M]	MO 13	MO 215, Brighton, MO	11/15/2019
29 [EB M]	MO 13	545th Road and MO 215, Brighton, MO	11/15/2019
30 [EB M]	MO 94	South Breeze Lane, Weldon Spring, MO	9/4/2019
31 [EB M]	MO 13	Route BB and Route CC, Alsup, MO	11/15/2019
32 [EB M]	MO 13	Route WW, Springfield, MO	11/15/2019
33 [EB M]	MO 13	State Highway O, Springfield, MO	11/15/2019
34	MO 13	South Farm Road 157, Springfield, MO	5/14/2020
35	US 50	Highway AA, Kingsville, MO	5/15/2020
36	US 50	Highway Z, Kingsville, MO	5/15/2020
37	US 61	1st Street, New London, MO	9/30/2020

#	Major Road	Minor Road	Installation
38	US 160	North Haseltine Road, Springfield, MO	12/1/2020
39	US 160	North Westgate Avenue, Springfield, MO	12/1/2020
40	US 60	Glendale Drive and Center Road, Rogersville, MO	10/19/2020
41	MO 30	Scottsdale Road, House Springs, MO	11/4/2020
42	US 63	East New Salem Lane, Ashland, MO	11/15/2021
43	US 63	Angel Lane and Minor Hill Road, Ashland, MO	11/15/2021
44	US 54	Midway Road and Jamie Lane, Eldon, MO	10/14/2022
45	US 54	Allen Road, Eldon, MO	10/14/2022
46	US 54	Highway FF, Eldon, MO	10/14/2022
47	US 67	Highway H, Farmington, MO	9/30/2022

[CG] – this J-turn was chosen for the CG analysis.

[EB] – this J-turn was chosen for the EB analysis.

[M] – this J-turn was chosen for the crash frequence modeling.

Table A-2. General Data for All J-turns in Missouri

#	# of lanes	Speed limit	AADT	Minor AADT	# of signs	# of access points
1	2	70	24,375 - 30,918	n/a	16	3
2	2	60	8,891 - 11,473	5,066 - 5,648	18	0
3	2	65	13,109 - 18,122	636 - 1,910	11	0
4	2	65	14,873 - 21,931	974 - 1,085	16	2
5	2	65	14,879 - 35,043	n/a	11	1
6	2	65	14,873 - 21,931	810 - 934	6	1
7	2	60	22,352 - 33,580	2,597 - 2,735	17	0
8	2	65	11,181 - 19,355	n/a	11	0
9	2	70	23,292 - 33,697	n/a	16	1
10	2	65	5,852 - 10,020	690 - 1,194	10	0
11	2	65	6,898 - 8,430	1,090 - 2,597	11	0
12	2	65	7,716 - 11,810	1,336 - 2,027	10	0
13	2	65	9,434 - 14,335	n/a	12	0
14	2	65	5,852 - 8,430	1,570 - 2,364	8	0
15	2	70	13,855 - 21,693	n/a	15	0
16	2	70	24,617 - 30,918	n/a	9	0
17	3	65	12,488 - 17,601	2,821 - 3,765	14	3
18	2	70	5,609 - 6,865	278 - 887	16	0
19	2	70	11,817 - 16,471	848 - 1,090	13	0
20	2	65	12,624 - 18,110	2,843 - 3,401	24	6
21	2	60	10,409 - 16,123	2,705 - 2,863	28	0
22	2	65	15,695 - 20,635	1,324 - 2,310	6	0
23	2	65	17,296 - 27,842	n/a	16	0
24	2	55	11,583 - 13,081	1,980 - 6,250	9	1
25	2	60	20,483 - 33,755	1,300 - 3,048	22	1
26	2	65	7,522 - 10,383	1,184 - 2,145	5	0
27	2	60	9,693 - 27,916	n/a	8	0
28	2	65	15,300 - 20,839	1,666 - 2,211	11	0
29	2	65	15,300 - 20,839	1,975 - 2,661	5	0
30	2	55	26,602 - 43,005	n/a	22	1
31	2	65	15,300 - 23,593	1,058 - 1,154	14	0
32	2	65	18,579 - 24,242	1,154 - 2,724	10	0
33	2	65	18,579 - 25,968	1,524 - 2,066	7	0
34	2	55	27,549 - 44,648	n/a	8	1
35	2	65	12,476 - 18,790	278 - 375	23	1
36	2	65	12,941 - 19,632	1,346 - 1,846	32	1
37	2	65	8,259 - 13,094	670 - 972	18	0
38	2	60	12,084 - 14,510	n/a	5	0
39	2	60	12,084 - 14,510	n/a	11	0

#	# of lanes	Speed limit	AADT	Minor AADT	# of signs	# of access points
40	2	65	18,839 - 22,637	976 - 1,462	22	1
41	2	60	17,960 - 26,334	9,821 - 17,538	26	0
42	2	70	14,776	n/a	8	1
43	2	70	14,776	n/a	9	0
44	2	60	10,711	n/a	6	0
45	2	60	10,711	n/a	7	1
46	2	60	7,403	n/a	6	1
47	2	60	6,916	n/a	13	0

Table A-3. Geometric Data for Highways on all J-turns in Missouri

#	# of U-turns	# of through lanes (eastbound or northbound/ westbound or southbound)	Presence of loon (eastbound or northbound/ westbound or southbound)	Presence of Left turn lane from the mainline (eastbound or northbound/ westbound or southbound)	Presence of left-turn offset (eastbound or northbound/ westbound or southbound)
1	2	2 / 2	0 / 0	0 / 0	x / x
2	2	2 / 2	0 / 0	0 / 0	x / x
3	1	2 / 2	0 / 0	0 / 1	x / 1
4	2	2 / 2	0 / 0	1 / 1	1 / 1
5	1	2 / 2	0 / 0	1 / 0	1 / x
6	1	2 / 2	0 / 0	0 / 1	x / 1
7	2	2 / 2	0 / 0	1 / 1	0 / 0
8	2	2 / 2	1 / 1	1 / 1	0 / 0
9	2	2 / 2	0 / 0	0 / 0	x / x
10	2	2 / 2	1 / 1	0 / 0	x / x
11	1	2 / 2	1 / 1	0 / 0	x / x
12	2	2 / 2	1 / 1	0 / 0	x / x
13	2	2 / 2	1 / 1	1 / 1	0 / 0
14	2	2 / 2	1 / 1	0 / 0	x / x
15	2	2 / 2	1 / 1	1 / 1	0 / 0
16	1	2 / 2	x / 0	0 / 0	x / x
17	2	2 / 2	1 / 1	1 / 1	1 / 1
18	2	2 / 2	1 / 1	0 / 0	x / x
19	2	2 / 2	1 / 1	1 / 1	1 / 1
20	2	2 / 2	1 / 1	1 / 1	0 / 0
21	2	2 / 2	1 / 1	1 / 1	1 / 1
22	2	2 / 2	1 / 1	1 / 1	1 / 1
23	1	2 / 2	1 / x	1 / 0	1 / x
24	1	2 / 2	0 / 1	1 / 1	1 / 1
25	2	2 / 2	1 / 1	0 / 1	x / 1
26	2	2 / 2	1 / 1	1 / 1	1 / 1
27	1	2 / 2	1 / x	0 / 1	x / 1
28	2	2 / 2	1 / 1	1 / 1	1 / 1
29	2	2 / 2	1 / 0	1 / 1	1 / 1
30	2	2 / 2	0 / 0	1 / 1	1 / 1
31	2	2 / 2	1 / 1	1 / 1	1 / 1
32	2	2 / 2	1 / 1	1 / 1	1 / 1
33	2	2 / 2	1 / 1	1 / 1	1 / 1
34	1	2 / 2	0 / 1	1 / 1	1 / 1
35	1	2 / 2	0 / 0	1 / 0	1 / x

#	# of U-turns	# of through lanes (eastbound or northbound/ westbound or southbound)	Presence of loon (eastbound or northbound/ westbound or southbound)	Presence of Left turn lane from the mainline (eastbound or northbound/ westbound or southbound)	Presence of left-turn offset (eastbound or northbound/ westbound or southbound)
36	2	2 / 2	1 / 0	1 / 1	1 / 1
37	1	2 / 2	1 / 0	1 / 1	1 / 1
38	1	2 / 2	1 / 0	0 / 0	x / x
39	2	2 / 2	1 / 1	1 / 1	1 / 1
40	1	2 / 2	0 / 0	1 / 1	1 / 1
41	2	2 / 2	0 / 0	0 / 0	x / x
42	1	2 / 2	1 / x	0 / 0	x / x
43	1	2 / 2	X / 1	0 / 0	x / x
44	2	2 / 2	1 / 1	0 / 0	x / x
45	2	2 / 2	1 / 1	0 / 0	x / x
46	1	2 / 2	0 / x	1 / 1	1 / 1
47	2	2 / 2	1 / 1	0 / 0	x / x

Note: In columns that indicate presence with the values 0, 1, and x, '0' corresponds to 'no', '1' to 'yes', and 'x' to 'not applicable'.

Table A-4. Geometric data for J-turn minor roads in Missouri

#	# of lanes on the minor road approach	Presence of a deceleration lane for turning right	Presence of an acceleration lane for turning right from minor road	Presence of a splitter island on the minor approach	Presence of median deceleration lanes	Presence of median acceleration lanes
1	2 / x	1 / x	0 / x	0 / x	1 / 1	1 / 1
2	1 / x	1 / x	0 / x	1 / x	1 / 1	0 / 0
3	2 / 2	1 / 0	1 / 0	1 / 0	1 / x	1 / x
4	2 / 2	1 / 1	1 / 1	0 / 1	1 / 1	1 / 1
5	x / 2	x / 1	x / 0	x / 0	0 / x	0 / x
6	2 / 2	0 / 1	0 / 0	0 / 0	0 / 0	0 / 0
7	1 / 1	1 / 1	1 / 1	0 / 0	1 / 1	1 / 1
8	1 / 1	1 / 1	0 / 0	0 / 1	1 / 1	0 / 1
9	2 / 2	1 / 1	1 / 1	0 / 0	1 / 1	1 / 1
10	1 / 1	1 / 1	0 / 0	1 / 1	1 / 1	0 / 1
11	1 / 1	1 / 1	0 / 0	1 / 1	1 / 1	1 / 1
12	1 / 1	1 / 1	0 / 0	1 / 1	1 / 1	0 / 1
13	1 / 1	1 / 1	1 / 1	0 / 1	1 / 1	0 / 1
14	1 / 1	1 / 1	0 / 0	1 / 1	1 / 1	1 / 1
15	2 / 2	1 / 1	1 / 1	1 / 1	1 / 1	1 / 1
16	2 / 2	1 / 1	0 / 0	0 / 0	X / 1	X / 1
17	1 / 1	1 / 1	1 / 0	1 / 1	1 / 1	1 / 1
18	1 / 1	0 / 1	0 / 0	0 / 0	1 / 1	0 / 0
19	1 / 1	1 / 1	0 / 0	1 / 1	1 / 1	0 / 1
20	1 / 1	1 / 1	1 / 1	1 / 1	1 / 1	1 / 1
21	1 / 1	1 / 0	0 / 0	1 / 1	1 / 1	0 / 0
22	1 / 1	1 / 1	1 / 1	1 / 1	1 / 1	1 / 1
23	x / 1	x / 1	x / 0	X / 0	1 / 1	0 / 0
24	1 / 1	1 / 1	0 / 1	0 / 1	0 / 1	0 / 1
25	2 / 2	1 / 0	0 / 0	1 / 0	1 / 1	1 / 1
26	1 / 1	1 / 1	0 / 1	1 / 1	1 / 1	1 / 1
27	2 / x	1 / x	1 / x	1 / x	1 / x	1 / x
28	1 / 1	1 / 1	1 / 1	1 / 1	1 / 1	1 / 1
29	1 / 1	1 / 1	1 / 0	1 / 0	1 / 1	1 / 0
30	1 / 1	1 / 1	0 / 0	1 / 1	1 / 1	0 / 1
31	1 / 1	1 / 1	1 / 1	1 / 1	1 / 1	1 / 1
32	1 / 1	1 / 1	1 / 1	1 / 1	1 / 1	1 / 1
33	1 / 1	1 / 1	1 / 1	1 / 1	1 / 1	1 / 1
34	1 / 1	0 / 0	0 / 1	1 / 0	0 / 1	0 / 1
35	1 / x	1 / x	1 / x	1 / x	0 / 1	1 / x
36	1 / 1	1 / 1	1 / 1	1 / 1	1 / 1	1 / 1
37	1 / 1	1 / 1	1 / 0	1 / 1	1 / 0	0 / 1
38	1 / 1	1 / 1	1 / 1	1 / 1	0 / 1	0 / 1
39	1 / 1	1 / 1	1 / 1	1 / 1	1 / 1	1 / 1

#	# of lanes on the minor road approach	Presence of a deceleration lane for turning right	Presence of an acceleration lane for turning right from minor road	Presence of a splitter island on the minor approach	Presence of median deceleration lanes	Presence of median acceleration lanes
40	1 / 1	0 / 0	1 / 1	1 / 1	1 / 1	1 / 1
41	1 / 1	0 / 1	1 / 1	1 / 1	1 / 1	0 / 0
42	2 / x	1 / x	1 / x	1 / x	1 / x	1 / x
43	2 / 2	1 / 1	1 / 1	0 / 0	X / 1	X / 1
44	2 / 2	1 / 1	0 / 0	1 / 1	1 / 1	1 / 1
45	2 / 2	1 / 1	0 / 1	1 / 1	1 / 1	1 / 1
46	2 / 2	1 / 1	1 / 1	1 / 1	1 / x	1 / x
47	1 / 1	1 / 1	0 / 0	0 / 1	1 / 1	1 / 1

Note: In columns that indicate presence with the values 0, 1, and x, '0' corresponds to 'no', '1' to 'yes', and 'x' to 'not applicable'.

Table A-5. Measured data for J-turns in Missouri.

#	Width of the median (feet)	Distance from the minor road to the downstream U-turn (feet)	Skew angle of the intersection (degree)	Horizontal curve radius at the intersection (feet)	Vertical grade at the intersection (feet)
1	44.3	1,423 / x	90.0	1,000,000	2.00%
2	47.3	1,873 / x	90.0	1,000,000	0%
3	823.0	1,691 / x	90.0	1,000,000	3.80%
4	62.0	1,952 /1,920	86.9	600	0.90%
5	59.7	1,967 / x	86.7	240	0.30%
6	57.4	1,446 /5,259	87.2	477.28	1.40%
7	49.0	1,471 /1,669	66.5	1,000,000	0.03%
8	49.2	986 /744	56.4	1,000,000	0%
9	58.6	3,031 /2,315	87.5	1433.36	2.10%
10	58.9	604 /583	84.3	1,000,000	0%
11	57.1	587 /590	90.0	1,000,000	0%
12	57.9	1,290 /602	89.6	1,000,000	0%
13	33.5	991 /1,082	85.2	1,000,000	0%
14	57.4	613 /626	89.1	1,000,000	0%
15	58.2	2,623 /2,934	75.0	1,000,000	0.40%
16	60.0	x/3,579	89.9	1,000,000	0.40%
17	60.2	2,342 /2,493	89.2	1,000,000	0%
18	57.2	2,304 /2,241	69.6	1,000,000	0%
19	46.6	2,029 /2,028	70.9	1,000,000	0%
20	63.4	3,485 /2,062	88.0	1,000,000	0%
21	58.6	1,611 /1,515	89.0	1,000,000	0%
22	60.7	1,589 /1,516	62.9	1,000,000	0%
23	23.5	x/1,349	89.6	1,000,000	0%
24	56.6	2,779 /1,154	88.4	1,000,000	1.70%
25	57.9	3,012 /2,637	79.7	1348.14	3.20%
26	56.1	1,340 /1,278	54.7	1,000,000	0%
27	56.3	151 / x	90.0	2864.8	1.10%
28	58.2	1,158 /1,145	88.8	1,000,000	2.10%
29	57.4	1,186 /3,213	86.5	1,000,000	0.70%
30	58.2	2,503 /3,192	100.1	1,000,000	0%
31	57.3	1,162 /1,086	95.1	1,000,000	1.00%
32	59.1	1,583 /1,487	89.3	1,000,000	0.50%
33	56.4	2,101 /2,025	89.8	1,000,000	0.20%
34	39.5	1,871 /1,388	85.3	1,000,000	0.30%
35	113.5	x/2,678	90.0	1,000,000	0%
36	92.0	2,719 /1,739	79.6	2864.79	0%
37	57.9	2,097 / x	80.3	5725.49	0%
38	57.8	x/4,249	63.1	1,000,000	0%
39	57.2	1,497 /1,439	90.0	1,000,000	1.90%
40	51.2	2,781 /1,807	71.1	1,000,000	0.50%

#	Width of the median (feet)	Distance from the minor road to the downstream U-turn (feet)	Skew angle of the intersection (degree)	Horizontal curve radius at the intersection (feet)	Vertical grade at the intersection (feet)
41	57.9	613 /703	82.5	1,000,000	0%
42	58.1	1,168 / x	90.0	1,000,000	1.50%
43	56.7	x/2,666	88.4	1,000,000	0.60%
44	61.4	2,994 /1,864	88.1	1,000,000	0.80%
45	59.7	3,518 /3,366	89.0	1910.4	1.40%
46	54.9	2102/x	84.5	2.863.87	0.12%
47	55.3	715/820	65.0	1,000,000	0%

Note: If there is no horizontal curve, the radius is recorded as 1,000,000. An 'x' value indicates that the feature is not applicable.